To the Graduate Council:

I am submitting herewith a dissertation written by Luo Cheng entitled "ADVANCED TECHNOLOGY FOR MEASURING WOOL TOP PROPERTIES." I have examined the final copy of this dissertation for form and content and recommend that it be accepted in partial fulfillment of the requirements for the degree of Doctor of Philosophy, with a major in Human Ecology.

Kermit E. Duckett

Kermit E. Duckett, Major Professor

We have read this dissertation
and recommend its acceptance.

M. A. Alst

Gajanan Bhat

R A Barr

Accepted for the Council:

Associate Vice Chancellor and
Dean of The Graduate School

Advanced Technology for Measuring Wool Top Properties

A Dissertation

Presented for the

Doctor of Philosophy

Degree

The University of Tennessee, Knoxville

Luo Cheng

December 1997

Copyright © Luo Cheng, 1997

All right reserved

DEDICATION

This dissertation is dedicated to my wife, Hsiao-Hwei Shen Cheng (沈曉慧), and my parents, Hong-Tao Cheng (程洪涛) and Qian-Juan Yang (楊钱娟).

ACKNOWLEDGEMENTS

I would like to express my great appreciation to my major advisor, Dr. Kermit E. Duckett, for the privilege of working with him, as well as the invaluable support and advice that he has given to me throughout this research. I extend thanks to Dr. Randall R. Bresee, Dr. Gajanan Bhat and Dr. Mongi A. Abidi for serving on my dissertation committee, reviewing this dissertation and teaching me so much throughout my graduate study.

Special thanks are extended to Mr. Hossein Ghorashi, senior vice president of Zellweger Uster Inc. for his support and encouragement. I sincerely thank Dr. Youe-T Chu for his help in understanding single fiber measurement and many helpful discussions. I am extremely appreciative to my colleagues, Mr. Joe Mansfield, Mr. Joe Baldwin, Mr. Masood Khan for mechanical design, setting up optical sensors and electronics, and selecting nozzles for fiber individualizer.

Finally, and most importantly, I would like to thank my wife, Hsiao-Hwei Shen Cheng, for her constant support and encouragement throughout my graduate study for pursuing Ph.D. degree.

ABSTRACT

Wool is an important textile fiber. The price of the wool is largely depending on fiber diameter, with length, vegetable matter and dark fiber content next. Numerous of individual instruments were developed to measure wool fiber properties but until now, there is no integrated fiber information system to measure major fiber properties. Therefore, it is desirable to develop an integrated system to measure wool fiber diameter, length and defects as HVI or AFIS used in cotton textile industry. The feasibility of this approach is discussed in this research project.

Using the latest technologies in digital signal and image processing, a research prototype instrument was developed. The instrument has an innovational design of a fiber individualizer based on drafting mechanism. Neural networks, fuzzy logic and genetic algorithms were applied to the waveform recognizer and defects classifier of the instrument and the results are discussed. Evaluated using a special set of wool samples, the instrument show promising results comparing with conventional individual instruments and human manual testing / inspection.

TABLE OF CONTENTS

CHAPTER PAGE

1. INTRODUCTION 1

1.1 MOTIVATIONS 1
1.2 NEURAL NETWORKS, GENETIC ALGORITHMS AND FUZZY LOGIC 1
1.3 MAJOR CONTRIBUTIONS OF THE THESIS 3
1.4 OUTLINE OF THE THESIS 4

2. REVIEW OF WOOL TESTING INSTRUMENT 6

2.1 WOOL FIBER PROPERTIES 6
2.1.1 Wool Fiber Structure and Properties 6
2.1.2 Top Properties 8
2.2 MAJOR INSTRUMENTS FOR WOOL TOP 10
2.2.1 Length Measurement 11
2.2.2 Diameter Measurement 13
2.2.3 Nep, Vegetable Matter and Dark Fiber Measurement 17

3. PATTERN RECOGNITION AND ARTIFICIAL INTELLIGENCE 19

3.1 INDUCTION OF DECISION TREE 21
3.2 NEURAL NETWORKS 22
3.2.1 Multi-layer Perceptron (MLP) 24
3.2.2 Probabilistic Neural Networks (PNN) 28
3.3 GENETIC ALGORITHMS 33
3.3.1 Representation 34
3.3.2 Creation of Initial Population 34
3.3.3 Genetic Operators 35
3.4 FUZZY LOGIC AND FUZZY REASONING 38
3.4.1 Fuzzy Set Theory 39
3.4.2 Basic Operations on Fuzzy Sets 39
3.4.3 Fuzzy Relations and Linguistic Variables 41
3.4.4 Fuzzy Reasoning 41

4. DESIGN OF THE NEW INSTRUMENT 44

4.1 REVIEW OF AFIS DESIGN 44
4.2 DESIGN OF THE NEW INSTRUMENT 46
4.2.1 Design of Sample Preparation Device 48
4.2.2 Design of Defects Detector 53
4.2.3 Design of Single Fiber Detector 54
4.2.4 Software Development 58

5. WOOL TOP LENGTH AND DIAMETER MEASUREMENT.....60
5.1 LENGTH AND DIAMETER MEASUREMENT FROM NORMAL SINGLE FIBER WAVEFORM 60
5.1.1 Length Models from the Waveform 60
5.1.2 Diameter Measurement 69
5.2 WAVEFORM ANALYSIS AND FEATURE SELECTION 69
5.2.1 Feature Selection 74
5.3 WAVEFORM RECOGNITION 75
5.3.1 Training and Testing Set 75
5.3.2 Waveform Recognition by Optimized Decision Tree 79
5.3.3 Waveform Recognition by Probabilistic Neural Networks 82
5.3.4 Discussions 84
5.4 OPTIMIZATION OF FIBER INDIVIDUALIZER 86
5.4.1 Experiment Design 86
5.4.2 Results 87
5.5 EVALUATION OF LENGTH AND DIAMETER MEASUREMENT 90
6. WOOL TOP DEFECTS INSPECTION 93
6.1 IMAGE PROCESSING AND MEASUREMENT 93
6.1.1 Preprocessing 93
6.1.2 Thresholding 96
6.1.3 Blob Labeling 97
6.1.4 Planer Shape Measures 97
6.2 OBJECT RECOGNITION AND FEATURE SELECTION 103
6.2.1 Object Recognition from a Noisy Background 103
6.2.2 Features for Dark-fiber and Vegetable Matter Classification 105
6.2.3 Features for Nep Classification 106
6.3 DEFECTS CLASSIFICATION 107
6.3.1 Training and Testing Samples 107
6.3.2 PNN Classifier 107
6.3.3 Fuzzy Logic Classifier 108
6.3.4 Results and Discussion 113
7. CONCLUSIONS AND RECOMMENDATIONS FOR FUTURE RESEARCH 116
7.1 CONCLUSIONS 116
BIBLIOGRAPHY 121
VITA 125

LIST OF FIGURES

FIGURE PAGE

FIGURE 2.1: WOOL FIBER STRUCTURE 7
FIGURE 2.2: PRINCIPLE OF AL-METER LENGTH MEASUREMENT 12
FIGURE 3.1: TYPICAL PATTERN RECOGNITION SYSTEM STRUCTURES. 20
FIGURE 3.2: STEPS INVOLVED IN THE DESIGN OF A TYPICAL PATTERN RECOGNITION SYSTEM 20
FIGURE 3.3: A BINARY TREE. 23
FIGURE 3.4: (A) A MULTI-LAYER PERCEPTRON. (B) A SINGLE NEURON. 25
FIGURE 3.5: (A) ORGANIZATION OF A PNN. (B) SINGLE NEURON OF THE PNN. 32
FIGURE 3.6: FLOW CHART OF A GA 36
FIGURE 3.7: FUZZY SETS. (A) "HIGH" FUZZY SET, (B) "LOW" FUZZY SET, (C) "AROUND" FUZZY SET 40
FIGURE 3.8: FUZZY APPROXIMATE REASONING 43
FIGURE 4.1: GENERAL SCHEMATIC OF AFIS 45
FIGURE 4.2: GENERAL SCHEMATIC OF THE NEW INSTRUMENT 47
FIGURE 4.3: DRAFTING UNIT USED IN SAMPLE PREPARATION DEVICE 50
FIGURE 4.4: PRINCIPLE OF INDIVIDUALIZATION BY DRAFTING 52
FIGURE 4.5: CAVITY ILLUMINATION. 55
FIGURE 4.6: INTEGRATING CYLINDER. 55
FIGURE 4.7: IMAGE OF ONE DARK FIBER AMONG MANY NORMAL FIBERS BY INTEGRATING CYLINDER 56
FIGURE 4.8: IMAGE ACQUISITION SYSTEM. 57
FIGURE 4.9: SINGLE FIBER DETECTOR. 59
FIGURE 4.10: DATA ACQUISITION SYSTEM 59
FIGURE 5.1: (A) FIBER AND SENSORS. (B) FIBER WAVEFORM FROM THE TWO SENSORS 61
FIGURE 5.2: T_B, T_E AND L. (A) T_B VS L, (B) T_E VS L 62
FIGURE 5.3: MLP CONFIGURATION. (A) MLP WITH LOGISTIC OR LINEAR ACTIVATION FUNCTION, (B) MLP WITH 2 SLABS IN HIDDEN LAYER, WITH GAUSSIAN AND GAUSSIAN COMPLIMENT ACTIVATION FUNCTION. 65
FIGURE 5.4: RESULTS FROM PHYSICAL AND EMPIRICAL MODELS. (A) PHYSICAL MODEL, (B) MLP MODEL WITH LOGISTIC ACTIVATION FUNCTION, (C) MLP MODEL WITH LINEAR ACTIVATION FUNCTION, (D) MLP MODEL WITH TWO SLABS IN HIDDEN LAYER. 68
FIGURE 5.5: LENGTH FROM PHYSICAL MODEL VS MLP_3 MODEL. 70
FIGURE 5.6: RESULTS OF LENGTH FROM MANUAL MEASUREMENT, PHYSICAL MODEL AND NEURAL NETWORK MODEL 71
FIGURE 5.7: DIAMETER MEASUREMENT FROM WAVEFORM. 72
FIGURE 5.8: TYPICAL WAVEFORMS. (A), (B) NORMAL SINGLE FIBER WAVEFORMS, (C) SINGLE FIBER WAVEFORM WITH LEFT SPIKE, (D) SINGLE FIBER WAVFORM WITH RIGHT. SPIKE, (E) LEFT-LOOP FIBER WAVEFORM, (F) RIGHT-LOOP FIBER WAVEFORM, (G) OVERLAP FIBER WAVEFORM, (H) BUNDLE FIBER WAVEFORM 73

FIGURE 5.9: FEATURES FROM WAVEFORM. 76
FIGURE 5.10: PEAK VOLTAGE DISTRIBUTION. 77
FIGURE 5.11: SHAPE FACTOR DISTRIBUTION. 78
FIGURE 5.12: FLOW CHART OF CLASSIFICATION. 80
FIGURE 5.13: EFFECT OF SMOOTHING FACTOR σ ON PNN CLASSIFICATION ERROR 84
FIGURE 5.14: COMPARISON OF LENGTH AND DIAMETER FROM NEW INSTRUMENT WITH AL-METER AND OFDA. 92
FIGURE 6.1: IMAGES OF DEFECTS AMONG NORMAL FIBERS, (A) DARK-FIBER, (B) STRAW, (C) SPECKS, (D) NEP. 94
FIGURE 6.2: FLOW CHART OF IMAGE PROCESSING AND ANALYSIS 95
FIGURE 6.3: THRESHOLDED IMAGES OF FIGURE 6.1 98
FIGURE 6.4: (A) 4-CONNECTIVITY, (B) 8 CONNECTIVITY. 99
FIGURE 6.5: EXAMPLE OF A LABELING PROCESS. 99
FIGURE 6.6: ILLUSTRATION OF AXIS RATIO AND FILLING FACTOR. 102
FIGURE 6.7: (A) RESULT OF CLUSTERING. (B) RESULT OF OBJECT RECOGNITION. 104
FIGURE 6.8: (A) CROSS-SECTION OF A LOOSE FIBER CLUSTER. (B) CROSS-SECTION OF A NEP. 108
FIGURE 6.9: ILLUSTRATION OF BLOB AREA A_1 AND ITS NEIGHBORHOOD AREA A_2. 108
FIGURE 6.10: FUZZY REASONING SYSTEM. 110
FIGURE 6.11: FUZZY REASONING FOR NEP. 112

LIST OF TABLES

TABLE PAGE

TABLE 3.1: ACTIVATION FUNCTIONS 26
TABLE 5.1: DECISION TREE CLASSIFICATION RESULTS FROM TESTING SET. 82
TABLE 5.2: PNN CLASSIFICATION RESULTS FROM TESTING SET 85
TABLE 5.3: LENGTH AND DIAMETER OF THE SAMPLE 88
TABLE 5.4: PARAMETERS OF DRAFTING DEVICE 88
TABLE 5.5: RESULTS FROM THE PRESSURE EXPERIMENT 88
TABLE 5.6: RESULTS FROM SPEED EXPERIMENT 88
TABLE 5.7: RESULTS FROM DRAFTING EXPERIMENT TO SHOW THE RELATIONSHIP BETWEEN THE FIRST AND SECOND DRAFTING ZONE. 89
TABLE 5.8: RESULTS FROM DRAFTING EXPERIMENT (TOTAL DRAFTING) 89
TABLE 5.9: LENGTH AND DIAMETER OF THE SAMPLES MEASURED BY NEW INSTRUMENT. . 91
TABLE 5.10: LENGTH AND DIAMETER OF THE SAMPLES MEASURED BY AL-METER AND OFDA. 91
TABLE 6.1: PNN CLASSIFICATION RESULTS FOR VEGETABLE MATTER FROM TESTING SET. 115
TABLE 6.2: FUZZY LOGIC CLASSIFICATION RESULTS FOR VEGETABLE MATTER FROM TESTING SET. 115
TABLE 6.3: FUZZY LOGIC CLASSIFICATION RESULTS FOR NEP FROM TESTING SET. 115

CHAPTER 1

INTRODUCTION

1.1 Motivations

Wool is an important textile fiber. About 70% of wool produced are consumed in apparel. Wool has dominated the formal wear market and, now, the use in knitwear and jackets are increasing. The price of the wool is largely depends on fiber diameter, with length, vegetable matter and dark fiber content next. Numerous individual instruments have been developed to measure wool fiber properties. But until now, there is no integrated fiber information system to measure major fiber properties. Especially, defects such as dark fibers, vegetable matter and neps are inspected by human operators, therefore, it is desirable to develop an integrated system to measure wool fiber diameter, length and defects as HVI or AFIS used in cotton textile industry. The feasibility of this approach is discussed here using advanced technologies.

1.2 Neural Networks, Genetic Algorithms and Fuzzy Logic

In recent years, there has been a growing interest in applying neural networks to pattern recognition, prediction and modeling. The most popular neural networks is a multi-layer perceptron trained by backpropergation algorithm which has powerful function-approximation capabilities. The probabilistic neural networks also have a solid theoretical basis. Under very general conditions, its ability to classify is asymptotically

Bayes-optimal. Neural networks are most likely to be superior to other methods under the following conditions:

- The data on which conclusions are to be based is "fuzzy" or the input data is subject to possibly large error or ill-defined categories.
- The data exhibits significant unpredictable nonlinearity.
- The input and output relationship can not easily be described by mathematical models.

Genetic algorithms are search algorithms based on the mechanics of natural selection and natural genetics. Genetic algorithms seek to solve optimization problems using the methods of evolution, specifically survival of the fittest. There are three basic genetic algorithm operators, namely, reproduction, crossover, and mutation. These three operators form the main body of the genetic algorithms. Genetic algorithms are theoretically and empirically proven to provide robust search in complex search space. Having been established as a valid approach for solving problems requiring efficient and effective search, genetic algorithms are now finding more widespread applications in business, scientific, and engineering fields. In a typical optimization problem, there are a number of variables, which control the process and a formula, which combines the variables to fully model the process. The problem is then to find the values of the variables that optimize the model in some way. If the model is a formula, then we will usually be seeking the maximum or minimum value of the formula. There are many mathematical methods which can optimize problems of this nature for fairly " well behaved" problems. These traditional methods tend to break down when the problem is not so well behaved. Examples of these types of problems include combinational

problems, or problems where the objective functions is not a smooth, continuous mathematical formula. In these cases, genetic algorithms are well suited to solve the problem.

Fuzzy modeling and reasoning has become a field of fruitful and intensive research in recent years. Fuzzy sets have been mainly used for express uncertainty and similarity. Fuzzy sets are convenient for representing incomplete or vague states of information under the form of possibility distributions. Fuzzy sets are also suitable for expression of closeness, proximity and similarity. The elements with membership 1.0 are viewed as prototypes of the fuzzy set, while the other membership grades estimate the closeness of the elements to the prototype. Moreover, the idea of similarity can be naturally graded by means of fuzzy relations.

It is important to understand the advantages, disadvantages, and the applications of neural networks, genetic algorithms and fuzzy logic. That is one of the goals of this effort.

1.3 Major Contributions of the Thesis

The major accomplishment of this research project is the design and development of an integrated instrument system to measure wool top properties. The applications of the latest technologies such as neural networks and genetic algorithms were explored throughout the development of the intelligent instrument. The prototype instrument show promising results comparing conventional individual instruments and human manual testing / inspection. Comparing to the existing instrument for cotton, Advanced Fiber Information System (known as AFIS), the major contributions are:

- Design of a new individualizer based on drafting mechanism that can individualize long staple fibers up to 300 mm with minimum fiber breakage.
- Design of a new waveform recognizer that can effectively reject bundle fibers and loop fibers based on advanced pattern recognition techniques.
- Using image analysis and pattern recognition technique to detect dark-fibers and vegetable matter in wool top.
- Using image analysis and pattern recognition technique to detect neps in wool top.

1.4 Outline of the Thesis

In Chapter 2, the major commercial instruments used in wool industry are briefly reviewed along with important wool properties that relate to pricing and influence on yarns and end products. A review of pattern recognition techniques and artificial intelligence is presented in Chapter 3 that include artificial neural networks, genetic algorithms and fuzzy logic. Chapter 4 discusses the design of new instrument that will measure wool fiber length, diameter and their distribution, as well as defects inspection such as dark fiber content, vegetable matter and neps. The focus of this chapter is an innovative sample preparation device that is the key to the success of the project. A probabilistic neural network classifier and an optimized decision tree classifier are developed to classify waveforms into measurable and non-measurable classes. The length and diameter will be measured on measurable single fiber waveforms. These developments and the results are discussed in Chapter 5. In Chapter 6, digital image processing and analysis will be applied to dark fiber, vegetable matter and nep inspection.

Various algorithms of shape analysis will be tried to classify defects into dark fibers, vegetable matter and neps. Probabilistic neural network and fuzzy logic classifiers will be discussed. Conclusions and recommendations will be presented in Chapter 7.

CHAPTER 2

REVIEW OF WOOL TESTING INSTRUMENT

2.1 Wool Fiber Properties

2.1.1 Wool Fiber Structure and Properties

The wool fiber consists of a roughly circular cylinder, tapering from the root to the tip, and with the complex structure illustrated in Figure 2.1. It normally occurs in a spirally crimped form. The bulk of the fiber is made up of a mass of cortical cells. In coarse wool, there may be a medulla at the center made up of a different type of cell, but in fine wool this is absent. At the surface of the fiber, there are cuticle cells or scales. These scales face towards the tip of the fibers and cause a directional effect, which is important in the frictional behavior of wool. Wool fibers vary in length from about 35 mm to 300 mm. Fine wool is usually from 35 mm to 125 mm long. Medium wool from 60 mm to 150mm, and coarse wool from 125 mm to 300 mm. Fine fibers such as Merino have an average diameter of about 15 to 17 microns; medium wool, from 24 to 34 microns; and coarse wool, about 40 microns. Some wool fibers are exceptionally stiff and coarse. These are called kemp. Wool fibers have a natural crimp. This crimp increases the elasticity and elongation of the fiber and also aids in yarn manufacturing. Compared to many other fibers, wool is weak. This weakness restricts the kinds of yarn and fabric

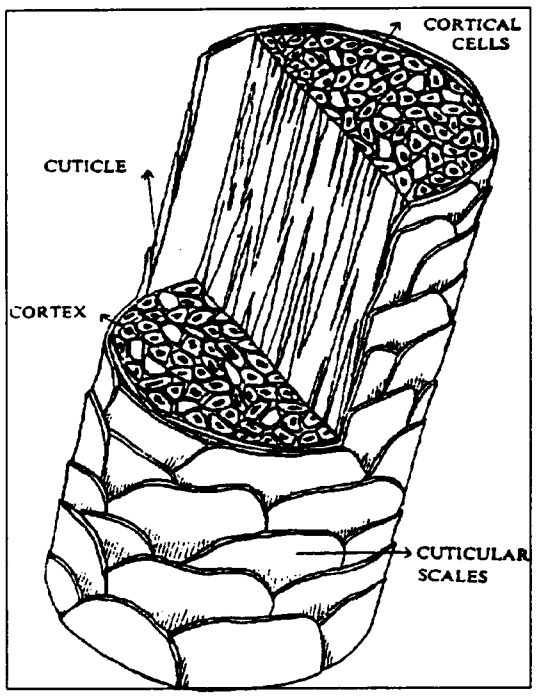


Figure 2.1: Wool Fiber Structure

constructions that can be used satisfactorily. However, other properties such as resiliency, elongation, and elastic recovery compensate for the low strength; they allow for production of wool yarns and fabrics that are durable. The elongation of wool is good; elastic recovery, very good; and resiliency, exceptionally good. As a result, wool fabrics will readily spring back into shape after crushing or creasing. The excellent resilience of wool fiber also gives it loft, which produces open, porous fabrics with good covering power or thick and warm fabrics. Wool will absorb moisture to a high degree - approximately 30 percent of its weight. Wool is easily dyed a wide of colors; it has good to excellent colorfastness when proper dyestuffs are used.

2.1.2 Top Properties

Usually, raw wool is processed into tops by wool top manufactures and spinners buy tops to spin into yarns. The important wool top properties are fiber diameter, fiber length, dark fiber content, vegetable matter and neps. These properties are discussed with respect to their importance in spinning and their effect on yarn properties.

Fiber Diameter and Distribution

Fiber diameter is the most important property of wool. For the spinner, the strength and uniformity of a yarn is very largely determined by the average number of fibers in the cross section. Fineness also plays an important part in determining the ease with which fibers can be twisted together during yarn formation. For a given yarn count, the finer the fibers, the more uniform is the yarn. Improved uniformity not only improves yarn appearance but also introduces other important consequences including greater strength, luster, fewer end-breakage in spinning, winding and greater resistance to surface

abrasion. A minimum number of fibers are required in the yarn cross section for satisfactory performance. Within the wool industry there is considerable interest in the relative importance of fiber diameter variability compared to mean fiber diameter. Anderson [1] defined an effective fineness as

$$F_e=D(1+5(CV\%/100)^2)^{0.5}, \qquad (2.1)$$

where D = mean fiber diameter and CV% = coefficient of variation of fiber diameter. This combines the mean diameter and coefficient of variation of diameter into a single measure of fineness. The applicability of the relationship between effective fineness and yarn evenness has been experimentally verified by Lamb[2].

Fiber diameter is also an important factor in determining the stiffness of a fabric or, alternatively, its softness of handle and its draping quality. The comfort of fabric against the skin is related to the number of fibers coarser than about 30 um present. For most people fabric is uncomfortable when the proportion of fibers coarser than 30 um exceeds 5 %.

Fiber Length and Length Distribution

Fiber length and length variability of top influence both the spinability of the top into yarn and the qualities of the yarn produced from the top. All else being equal, yarns spun from longer fibers will have reduced ends down during spinning. Longer fibers tend to produce more even, stronger and more extensible yarns also. Lower CV% appears to be related to increased yarn strength.

Dark or Colored Fibers

Top or yarn with a dark fiber content that is too high (for example more than 100 dark fibers per kg of top) may be heavily discounted. If it is spun and made into fabric before discovery it may lead to expensive repairs to remove the fibers from the fabric.

Faults in Slivers

Both neps and small pieces of vegetable matter in the top will interfere with spinning and cause ends down as their presence may reduce the number of fibers present at points along the yarn. Neps and vegetable matter that survive in the yarn will produce unacceptable faults. A nep is likely to lead to a thick place in the yarn while vegetable matter may result in an unsightly piece that dyes differently to the host wool.

2.2 Major Instruments for Wool Top

The International Wool Textile Organization (IWTO) is an Association of organizations interested in the merchandising, processing, spinning and weaving of wool and allied fibers under private enterprise. The IWTO Red Book is the collective test methods that have been developed over the years by the Working Groups of the IWTO Technical Committee. IWTO Test Methods are available for the measurement of a wide range of wool products and a wide range of properties. All instruments should be certified by IWTO.

2.2.1 Length Measurement

Fiber length measurements were originally made using comb sorters, which sorted fibers into length groups. AL-Meter is an automated comb sorter. As specified by IWTO test method (IWTO-17-85) [3], the AL-Meter is an electronic apparatus for measuring the length of wool fibers, working with a specimen of fibers built-up using a preparatory machine called the "Fibroliner". This test specimen is arranged in the form of a sheet of fibers, with all the fibers having one of their ends situated approximately on the same line, perpendicular to the direction of the fibers. The specimen so formed is then transferred from the Fibroliner to the electronic apparatus, where it is inserted between two plastic sheets supported by a sliding carriage. The carriage, containing the test specimen, is moved at constant speed through a capacitance sensor as shown in Figure 2.2. The variation in capacitance so produced is proportional to the mass of the portion of the fibrous sheet between the plates of the condenser. Knowing the formation of the sample, it can be shown that the measured signal is equivalent to a cumulative "HAUTEUR" (H) diagram (Staple Diagram). AL-Meter gives the following results:

- Length distribution biased by number (HAUTEUR).
- Length distribution biased by weight (BARBE).
- Mean length and CV% of HAUTEUR or BARBE.
- Percentage of fibers longer or shorter than a given length.
- Length exceeded by a specified percentage of the fibers.

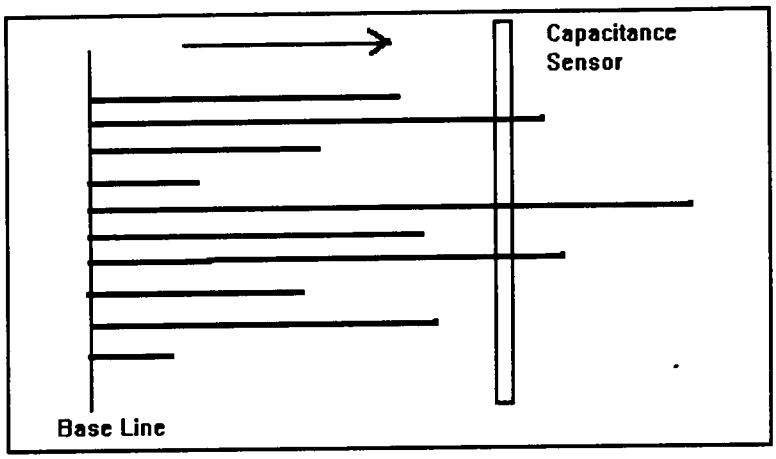


Figure 2.2: Principle of AL-meter Length Measurement.

Barbe is the length calculated from the average of the weight of fibers of each length class in a numeric sample obtained from a comb sorter. Let $w(l) \bullet \Delta l$ be the weight of fibers in the length interval from l to $l+\Delta l$. Then $\sum w(l) \bullet \Delta l$ is the total weight of fibers present over all lengths. Then barbe (B), the weight biased mean fiber length may be calculated from:

$$B = \frac{\sum w(l) \bullet l \bullet \Delta l}{\sum w(l) \bullet \Delta l} \qquad (2.2)$$

Hauteur is the length calculated from the number of fibers of each length class in a numeric sample. Let $n(l) \bullet \Delta l$ be the number of fibers in the length interval from l to $l + \Delta l$. Then $\sum n(l) \bullet \Delta l$ is the total number of fibers present over all lengths. Then hauteur (H), the number-biased fiber length may be calculated from:

$$H = \frac{\sum n(l) \bullet l \bullet \Delta l}{\sum n(l) \bullet \Delta l} \qquad (2.3)$$

2.2.2 Diameter Measurement

The major instruments for wool fiber diameter measurement are OFDA (IWTO-47-95) [4], LaserScan (IWTO-12-95) [5], AirFlow Apparatus (IWTO-6-92) [6] and Projection Microscope (IWTO-8-89) [7].

The measurement of the diameter of wool fibers in top has been carried out for commercial purposes for many years. Initially the methods used were microscopic, measuring fiber cross-section or longitudinal section. IWTO had started trying to standardize procedures in the late 1930s. Microscopic measurement techniques are tedious however, as several hundred fibers need to be measured to obtain a satisfactory

measurement precision. In the late 1930s and early 1940s researchers realized that an air-flow method could be used to obtain the mean fiber diameter of samples of wool. Air-flow measurement became generally popular during the 1950s and 1960s for use with top. Continued research into procedures for the rapid measurement of fiber diameter and its distribution have resulted in a number of instruments being developed such as Laserscan and OFDA which use Electro-optics sensors and CCD camera respectively.

Projection Microscope

Projection microscope is a reference method for wool fiber diameter measurement. Magnified images of the profiles of short length of fiber are projected on a screen and their widths measured by using a graduated scale. The individual fiber measurements are recorded and when sufficient fibers have been measured the mean, standard deviation, and coefficient of variation of the fiber diameter distribution are calculated. A histogram may be drawn.

AirFlow Apparatus

Before the invention of Laserscan and OFDA, airflow apparatus were used for wool fiber diameter measurement. A specified mass of wool is compressed to a constant volume in a cylindrical chamber with perforated ends to which a flowmeter and a manometer are connected. A regulated current of air is then passed through the compressed fibers and the mean fiber diameter is derived from the manometer or the flowmeter reading. Airflow apparatus only give the mean fiber diameter in micrometers. The air-flow method relies on Kozeny's Law which relates the flow of a fluid through a porous sample to the change in pressure across the sample.

$$Q = f(\Delta P/R) \qquad (2.4)$$

Where Q is the fluid flow, ΔP is the pressure change; R is the resistance to flow of a specimen. For a given specimen mass, wool samples of finer diameter offer greater resistance. Therefore for a fixed pressure drop, Kozeny's Law may be expressed as:

$$Q = f(1/d) \qquad (2.5)$$

where d is diameter. An increase in fiber diameter will allow greater air flow through the specimen.

Sirolan-Laserscan Fiber Diameter Analyzer

The FDA was developed during the early 1970s at CSIRO Division of Textile Physics. It was designed to give a rapid measurement of fiber diameter distribution by passing fiber snippets past a laser light beam and measuring the shadow formed. The FDA has problems with the distribution results produced. False readings of crossed fibers and other artifacts were regularly interpreted as being real fibers, in spite of the techniques employed to discount them. In the early 1990s the CSIRO undertook a research program to redesign the FDA to eliminate metrology problems. This lead to the Laserscan that gave significantly superior results but still used the same basic technology.

Sirolan-Laserscan is an Electro-optics instrument. Snippets are cut from samples of raw wool, sliver or top and are cleaned where required. The snippets are dispersed as a dilute suspension in a mixture of propan-2-ol and water. The suspension of snippets is transported through a measuring cell that is positioned in a beam of laser light. The reduction in intensity of the laser beam as the individual snippets pass through the beam of light, approximately 500 micrometers in diameter, is sensed by a detector and

transformed, using a calibration look-up table, into a diameter in micrometers. A computer is used to collect and summarize the individual measurements to give statistics such as mean and standard deviation of fiber diameter for the specimen. Sirolan-Laserscan gives the following results:

- The mean fiber diameter in micrometers to one decimal place.
- The coefficient of variation of fiber diameter as a percentage to the nearest whole number.
- The distribution of fiber diameter as histogram.
- The Laserscan have a number of features which are designed to reject false readings, such as two fibers in the measurement zone, or small particles being interpreted as fiber. This may limit the number of accepted counts to about 40-50% of all registrations.

Optical Fiber Diameter Analyzer (OFDA)

Image analysis has been used to measure the diameter of fiber snippets starting with the Millipore PiMc. However it is only in recent years that the technology has allowed a viable instrument to be developed. The OFDA was developed by an Australian company, BSC Electronics.

OFDA is an automated microscope measurement. Snippets are cut from conditioned samples of raw wool or sliver. The snippets comprising a test specimen are spread uniformly over the surface of a microscope slide. A cover slide is placed over the specimen and the slide placed on a microscope stage, which is moved under computer control. The slide is stepped through the field of view of a low power objective. At each

step, the video system is instructed to capture and analyze a fiber image frame. Each diameter measurement is allocated to a diameter class and at the completion of the slide, the class contents are statistically analyzed to produce the mean and standard deviation of the diameter for the specimen. OFDA gives the following results:

- The mean fiber diameter in micrometers to one decimal place.
- The coefficient of variation of fiber diameter as a percentage to the nearest whole number.
- The distribution of fiber diameter as histogram.

2.2.3 Nep, Vegetable Matter and Dark Fiber Measurement

IWTO Method

The CSIRO Dark Fiber Detector (IWTO (E)-13-88) [8] is an illumination device used to detect dark fibers. The test specimen held between glass plates is placed on the instrument, and, the top and bottom illumination is balanced at the fiber plane. Dark fibers are assessed against reference fibers for darkness. If a fiber is sufficiently dark and meets the minimum length requirement (usually longer than 10 mm) it is recorded. Dark fibers may also be removed from the web for more detailed examination. A similar illumination device is used for top faults detection. For vegetable matter detection, the specimen is illuminated from behind (IWTO-24-73) [9]. For nep detection, a removable black screen is inserted. The following faults may be detected using this method:

- straws and bast fibers between 3 and 10 mm;
- straws and bast fibers greater than 10 mm;
- burrs (or fragments between 3 and 10 mm;

- burrs greater than 10 mm;
- colored fibers;
- slubs;
- loose slubs;
- neps .

ASTM Method

As specified by ASTM test method (ASTM D1770-88) [10], the nep, vegetable matter and colored fiber are measured manually. Four test specimens are taken and examined in accordance with specified procedures. Each observed nep or piece of vegetable matter is classified by size, by visual comparison with a specified standard size chart. The numbers of each class of neps and vegetable matter pieces, and the number of colored fibers, are recorded for each specimen. From these data the average counts per specimen of 15 g are calculated.

CHAPTER 3

PATTERN RECOGNITION AND ARTIFICIAL INTELLIGENCE

Pattern recognition (PR) techniques are often an important component of intelligent systems and are used for both data processing and decision making. Broadly speaking, pattern recognition is the science that concerns the description or classification (recognition) of measurements. PR is not comprised of one approach, but rather is a broad body of often loosely related knowledge and techniques. Historically, the two major approaches to pattern recognition are the statistical and syntactic approaches. Statistical PR assumes, as its name implies, a statistical basis for classification algorithms. A set of characteristic measurements, denoted features, is extracted from the input data and is used to assign each feature vector to one of the classes. It would be expecting too much to ask a classification system to be correct all of the time. Errors will, of course, be made. One goal of any classifier is to minimize the number of errors made, or to maximize the likelihood of making a correct class assignment. This can be done using probability theory. Recently, the emerging technology of neural networks has provided a third approach, especially for 'black box' implementation of PR algorithms. The structure of a typical pattern recognition system is shown in Figure 3.1. Notice that it consists of a sensor, a feature extraction mechanism (algorithm), and a classification algorithm. A flow chart of the process of designing a learning machine for pattern recognition is illustrated in Figure 3.2.

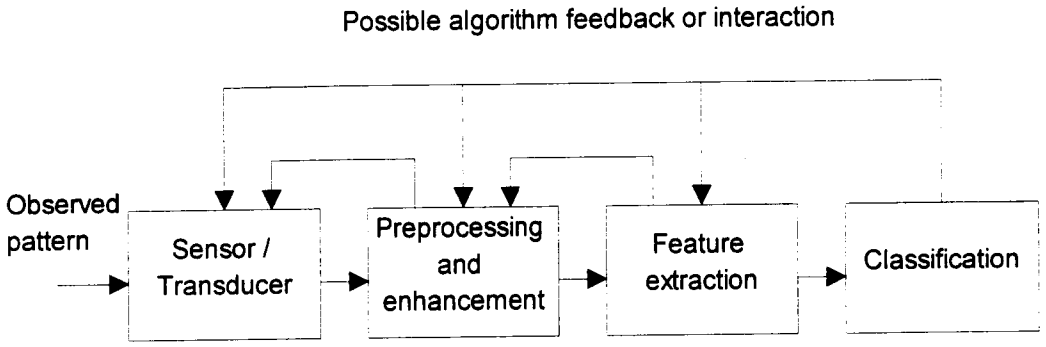


Figure 3.1: Typical pattern recognition system structures.

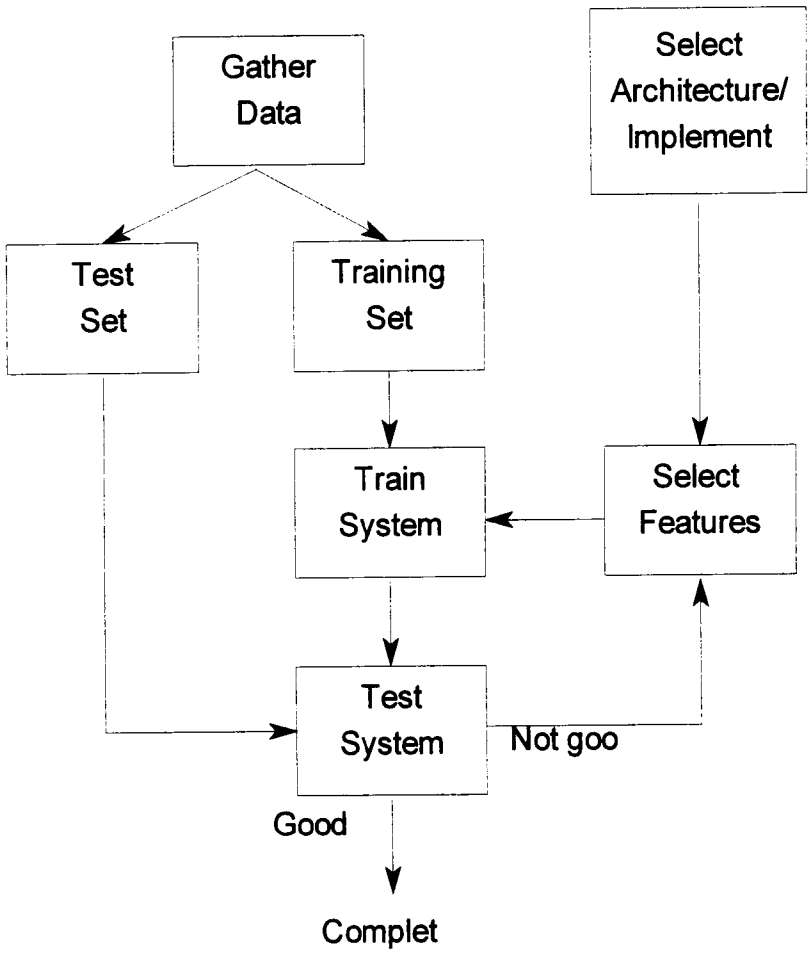


Figure 3.2: Steps involved in the design of a typical pattern recognition system.

Pattern recognition, naturally, is based on patterns. A pattern can be as basic as a set of measurements or observations in one dimensional such as waveforms or two-dimensional such as images. Features are any extractable measurement used. Note that: (1) significant computational effort may be required in feature extraction; and (2) the extracted features may contain errors or noise. It is important that the extracted features be relevant to the PR task at hand.

Artificial intelligence (AI) is a branch of computer science that studies how smart a machine can be, which involves the capability of a device to perform functions normally associated with human intelligence, such as reasoning, learning, and self-improvement. The field of artificial intelligence is composed of several areas of study. Expert systems are AI's first commercially viable product. In recent years, neural networks, genetic algorithms and fuzzy logic are the hottest topics in AI. These topics are briefly reviewed here and the applications in developing an intelligent instrument for wool are described in Chapter 5 and 6.

3.1 Induction of Decision Tree

A decision tree is a tree-structured classification strategy. Starting from a root node, it evaluates an attribute of an object and goes to one of the partition branches associated with the node according to the value of the attribute. If the branch leads to a terminal node or leaf, the category of the object is denoted by the class label attached to the leaf. If the branch leads to another node, the evaluation process continues until a leaf is reached. Induction of decision trees is a general purpose machine learning method developed independently by L. Breiman[11] and J.R.Quinlan[12]. It is a simple and

widely used symbolic algorithm to construct a decision tree from training example [13]. Each training example includes a set of attribute values and a category value. A training set is a collection of such examples. After being trained from training set, the algorithm is able to induce a decision tree that can correctly assign a new object to one of the prespecified categories. The training set must contain representatives of a real process in order to induce a decision tree that can extract internal relationships between the category and the attribute values of a pattern. After a decision tree is constructed, it is tested to see whether it can correctly classify all the patterns in the training set. If so, the decision tree is accepted and the process terminates. Figure 3.3 illustrates a binary tree where at each node there are only two partitions. A threshold is associated with each node that is used to compare with the most informative attribute. The decision goes to either of the two branches associated to the node according to the result of the comparison. When the terminal node is reached, the classification is complete and a label is obtained which represents the class of the pattern processed.

3.2 Neural Networks

This section begins a review of artificial neural networks (ANN) by examining the basic building blocks of ANN. ANN provide an emerging paradigm for pattern recognition implementation that involves large interconnected networks of relatively simple units (neural nets). ANN research has a rich history of approximately 40 years; however, it seems to be presently at an all-time peak.

Biological systems implement pattern recognition computations via interconnections of physical cells called neurons. This provides motivation to consider

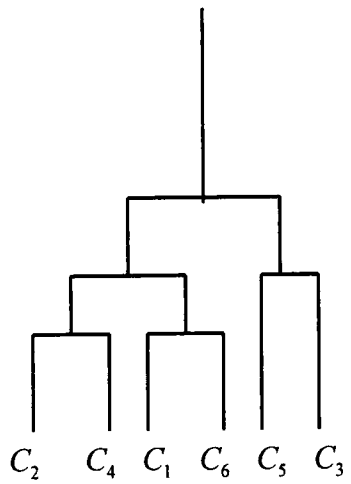


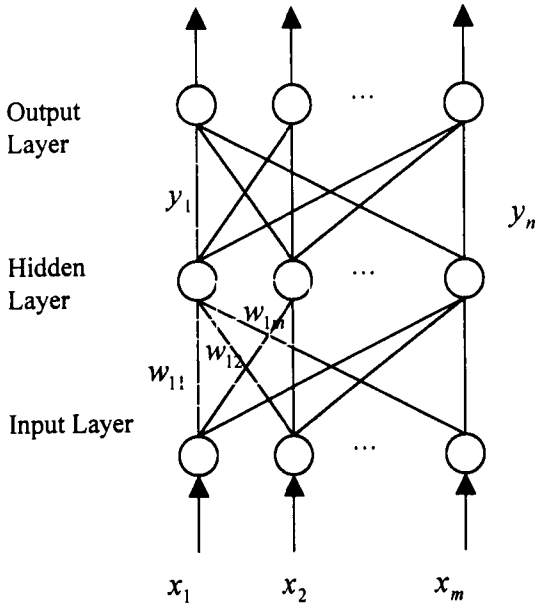
Figure 3.3: A Binary Tree.

emulation of this computational mechanism for automated PR applications. In fact, a whole field of study, centered around the creation and study of intelligent systems by recreating the computational structures of the human brain, has fully emerged in only the last decade.

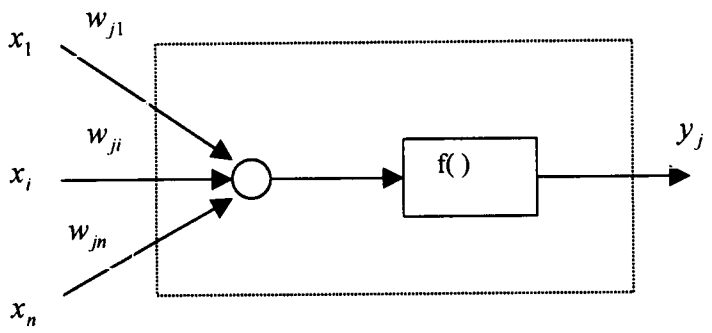
To some extent, the ANN approach is a nonalgorithmic, black box strategy, which is trainable. We hope to 'train' the neural black box to learn the correct response or output for each of the training samples. This strategy is attractive to the PR system designer, since the required amount of *a priori* knowledge and detailed knowledge of the internal system operation is minimal. Furthermore, after training we hope that the internal structure of the artificial implementation will self-organize to enable extrapolation when faced with new, yet similar, patterns on the basis of 'experience' with the training set. Learning in neural networks may be either supervised or unsupervised [14-18]. An example of supervised learning in a feedforward network is the backpropagation algorithm [19-20]. Unsupervised learning in a feedforward network is exemplified by the Kohonen self-organizing network [21].

3.2.1 Multi-layer Perceptron (MLP)

MLP is perhaps the best known type of feedforward networks. Figure 3.4 shows an MLP with three layers: an input layer, an output layer and a hidden layer. Neurons in the input layer only act as buffers for distributing the input signal x_i to neurons in the hidden layer. Each neuron j in the hidden layer sums up its input signals x_i after weighting



(a)



(b)

Figure 3.4: (a) A multi-layer Perceptron. (b) A single neuron.

them with the strength of the respective connections w_{ji} from the input layer and computes its output y_j as a function f of the sum

$$y_j = f\left(\sum w_{ji} x_i\right) \qquad (3.1)$$

f can be a simple linear, a sigmoid, or hyperbolic tangent function as shown in table 3.1. The output of neurons in the output layer is computed similarly.

The backpropagation algorithm, a gradient descent algorithm, is the most commonly adopted MLP training algorithm developed by Rumelhart *et al* [20]. It gives the change Δw_{ji} on the weight of a connection between neurons i and j as follow:

$$\Delta w_{ji} = \alpha \delta_j x_i \qquad (3.2)$$

where α is a parameter called the learning rate and δ_j is a factor depending on whether neuron j is an output neuron or a hidden neuron. For output neurons,

$$\delta_j = \left(\frac{\partial f}{\partial net_j}\right)\left(y_j^{(t)} - y_j\right) \qquad (3.3)$$

and for hidden neurons,

$$\delta_j = \left(\frac{\partial f}{\partial net_j}\right)\sum_q w_{qj}\delta_q \qquad (3.4)$$

Table 3.1: Activation functions

Type of Functions	Functions
Linear	$f(x)=x$
Sigmoid	$f(x)=1/(1+exp(-x))$
Hyperbolic tangent	$f(x)=(1-exp(-2x))/(1+exp(2s))$

In equation (3.3), net_j is the total weighted sum of input signals to neuron j and $y_j^{(l)}$ is the target output for neuron j.

As there are no target outputs for hidden neurons, in Equation (3.4), the difference between the target and actual output of a hidden neuron j is replaced by the weighted sum of the δ_q terms already obtained for neurons q connected to the output of j. Thus, iteratively, beginning with the output layer, the δ term is computed for neurons in all layers and weight updates determined for all connections. The weight updating process can take place after the presentation of each training patterns (pattern-based training) or after the presentation of the whole set of training patterns (batch training). In either case, a training epoch is said to have been completed when all training patterns have been presented once to the MLP.

In order to improve convergence of the algorithm it is possible to add a momentum term to the weight update. This means that the present update not only depends on the errors but also on the last update of that weight. Each weight in the network then has a momentum value associated with the last update, thus

$$\Delta w_{ji}(k+1) = \alpha \delta_j x_i + \mu \Delta w_{ji}(k) \qquad (3.5)$$

where $\Delta w_{ji}(k+1)$ and $\Delta w_{ji}(k)$ are weight changes in epochs (k+1) and (k), respectively, and μ is the momentum coefficient.

MLP is the most popular neural network model and has a wide range of applications that include classification, autoassociation, time-series prediction and function approximation.

3.2.2 Probabilistic Neural Networks (PNN)

Bayes Theorem

It has been assumed that the measurements of a particular feature will not be identical and will follow the normal distribution. It has also been assumed that there are a known number of classes to be dealt with and some classes will have higher probability than others will. To perform a classification based on the idea of maximum likelihood it is necessary to compute the value of $p(c_i|\vec{x})$, or the probability that an object belongs to class i given that we have a feature vector $\vec{x}$. The procedure would be to simply compute this vector for all classes and choose the class having the highest probability. The approach will use Bayes theorem. The *a priori* estimate of the probability of a certain class is converted to the *a posteriori*, or measurement conditioned, probability via

$$p(c_i|\vec{x}) = \frac{p(\vec{x}|c_i)p(c_i)}{p(\vec{x})} \qquad (3.6)$$

where $p(c_i|\vec{x})$ is the probability that an object belongs to class i given that a feature vector $\vec{x}$, $p(\vec{x}|c_i)$ is the probability of feature vector $\vec{x}$ given a class c_i, $p(c_i)$ is the probability of class i, $p(\vec{x}) = \sum_i p(\vec{x}|c_i)$.

This is helpful because $p(\vec{x}|c_i)$ and $p(c_i)$ are easier to estimate from data samples than is $p(c_i|\vec{x})$. The value of $p(\vec{x})$ is not important, since it will cancel out in most cases. The maximum likelihood classifier, or Bayes classifier, now involves computing $p(\vec{x}|c_i)\,p(c_i)$ for all classes i and assigning the sample to the class having the largest value of this expression. Baysian classification theory provides the foundation for the

probabilistic neural networks. It has been proven that the probabilistic neural network (PNN) approaches the Baysian classifier if the training set is large. This is the only artificial neural network to give such a guarantee. Furthermore, the PNN trains rapidly without the pathologies associated with backpropagation.

Parzen Windows

The Parzen-window approach to estimating densities can be introduced by assuming that region R_n is a d-dimensional hypercube. If h_n is the length of an edge of that hypercube, then its volume is given by

$$V_n = h_n^d \qquad (3.7)$$

The density estimation can be expressed as

$$P_n(\vec{x}) = \frac{1}{n}\sum_{k=1}^{n}\frac{1}{V_n}\varphi\left(\frac{\vec{x}-\vec{x}_i}{h_n}\right) \qquad (3.8)$$

where $\varphi(\ )$ is a window function. In essence, the window function is being used for interpolation, each sample contributing to the estimate in accordance with its distance from $\vec{x}$. It can be proven that

$$\lim_{n\to\infty}\overline{P}_n(\vec{x}) = p(\vec{x}) \qquad (3.9)$$

which means that when sample size is large, the estimate is close to true PDF.

Probabilistic Neural Networks

Recall the Bayes theory discussed in the previous section, assign sample $\vec{x}$ to class c_i if

$$p(c_i|\vec{x}) > Max(p(c_j|\vec{x})) \qquad i \neq j \qquad (3.10)$$

while this procedure leads to a theoretically optimal classification, determining $p(\vec{x}|c_i)$ usually presents practical difficulties. There are seldom enough samples to be available to cover all possible values of $\vec{x}$. Hence, some approximation must be used in the n dimensional PDF vector space. A powerful nonparametric estimator described by Pazzen is used in the PNN. Parzen proved that the sum of scaled n dimensional Gaussians would, in the limit, approximate the true PDF [22]. Thus, for each training example, a unit area n dimensional Gaussian is constructed in the PDF vector space for the correct class. This process is repeated for each training vector; then the estimated PDF is obtained by dividing the sum of these Gaussians by the number of vectors in that class. The resulting sum approaches the true PDF as the number of training vectors becomes large. The Gaussian function has the parameter σ that determines the spread of the function. σ can have a large effect on the accuracy of the approximation and should be scaled to the density of the samples. Typically, it will be set to smaller values for larger sample sizes. It is not necessary to calculate the full PDF when using Parzen windows for classification; all that is needed is its value at the sample vector point. The following equation expresses the method for finding the needed value for the PDF, extended to the n dimensional case:

$$p(\vec{x}|c_i) = \frac{1}{(2\pi)^{q/2}\sigma^q n}\sum_{j=0}^{n-1} e^{-\frac{\|x-x_j\|^2}{2\sigma^2}} \qquad (3.11)$$

where $p(\vec{x}|c_i)$ is the value of the PDF at the point specified by the sample vector $\vec{x}$. q is the number of components in the sample vector. σ is the smoothing variable and n is the number of sample vectors in class c_i. This equation may appear complicated, the idea is simple; just add up the value of the n dimensional Gaussians, evaluated at the training

vector point in n dimensional space and scale the sum to produce the estimated value of the PDF at that point. As the number of training vectors increases, the estimated PDF approaches the true value.

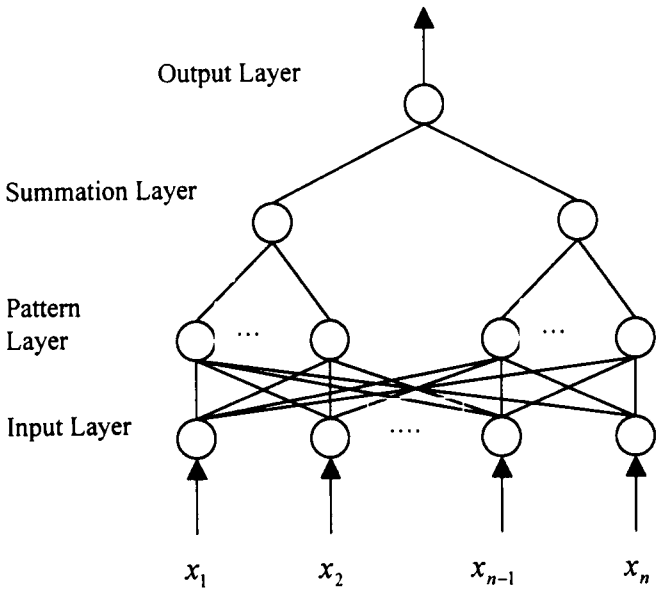
Specht [23-26] adapted this technique in 1988 to implement an artificial neural network. To do so, the sample vectors are normalized to unit length, thereby making them points on the unit hypersphere. A single neuron is plotted in Figure 3.5 (b). Input signals from the input units pass to the pattern units, each of which forms a dot product of the input vector $\vec{x}$ with a weight vector $\vec{w}_i$,

$$U_i = \vec{x} \cdot \vec{w}_i \qquad (3.12)$$

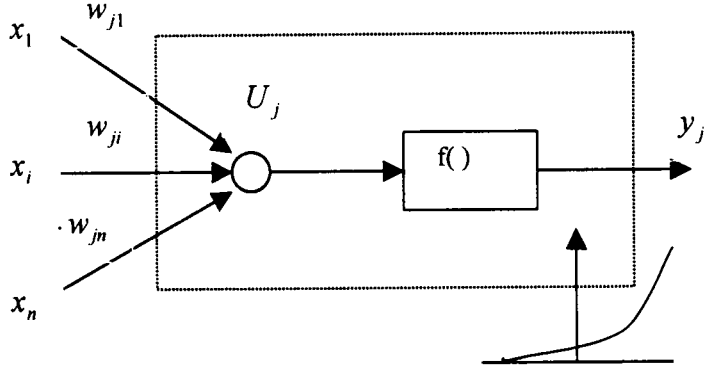
An exponentiation function is applied to U_i and the result is transmitted to the summation units. The exponential function can be represented as

$$f(U_i) = \exp\left[\frac{-(\vec{w}_i - \vec{x})'(\vec{w}_i - \vec{x})}{2\sigma^2}\right] \qquad (3.13)$$

where σ is a smoothing parameter. One such neuron is created for each training vector; thereby forming the network of Figure 3.5 (a). Here the input units are distribution points doing no processing; the pattern units are as described in the previous paragraph. The summation units sum over-all vectors in a given class, therefore producing a function proportional to the PDF for that class. The output units then perform pair-wise comparisons of the summation unit outputs, putting out class label depending upon which input is greater. The network is trained by setting the weight vector $\vec{w}_i$ in one of the pattern units equal to each $\vec{x}$ pattern in the training set. The pattern unit's output is then connected to the appropriate summation unit [24].



(a)



(b)

Figure 3.5: (a) Organization of a PNN. (b) Single neuron of the PNN.

PNN is fairly specialized, not having the wide applicability of the MLP. PNN is intrinsically a classifier and the advantage of this network model is that a byproduct of its computations is Bayesian posterior probabilities. If we need confidence estimates for the network's decisions, this model is a strong candidate. Another advantage is that the training speed is much faster than MLP.

3.3 Genetic Algorithms

A genetic algorithm (GA) is a directed random search technique, invented by Holland [27], which can find the global optimal solution in complex multi-dimensional search spaces. A GA is modeled on natural evolution in that the operators it employs are inspired by the natural evolution process. These operators, known as genetic operators, manipulate individuals in a population over several generations to improve their fitness gradually [28-32]. As discussed in the next section, individuals in a population are likened to chromosomes and usually represented as strings of binary numbers.

The evolution of a population is described by the "schema theorem". A schema represents a set of individuals in terms of the similarity of bits at certain positions of those individuals. A schema is characterized by two parameters: defining length and order. The defining length is the length between the first and last bits with fixed values. The order of a schema is the number of bits with specified values. The distribution of a schema through the population from one generation to the next depends on its order, defining length and fitness.

GA does not use much knowledge about the problem to be optimized and do not deal directly with the parameters of the problem. Thus, the first issue in a GA application

is how to code the problem under study. The second issue is the creation of a set of possible solutions at the start as the initial population. The third issue in a GA application is how to select a suitable set of genetic operators. Finally, as with other search algorithms, GA have to know the quality of already found solutions to improve them further.

3.3.1 Representation

The parameters to be optimized are usually represented in a string form since genetic operators are suitable for this type of representation. There are two common representation methods for numerical optimization problems. The preferred method is the binary string representation method. The reason for this method being popular is that the binary alphabet offers the maximum number of schemata per bit compared to other coding techniques. The second method is to use a vector of integers or real numbers with each integer or real number representing a single parameter. When a binary representation scheme is employed, an important step is to decide the number of bits to encode the parameters to be optimized. Each parameter should be encoded with the optimal number of bits covering all possible solutions in the solution space.

3.3.2 Creation of Initial Population

At the start of optimization, a GA requires a group of initial solutions. There are two ways of forming this initial population. The first consists of using randomly produced solutions created by a random number generator. The second method employs knowledge about the given optimization problem. Using this knowledge, a set of *a priori* requirements is obtained and solutions that satisfy those requirements are collected to

form an initial population. In this case, the GA starts the optimization with a set of approximately known solutions and therefore convergence to an optimal solution takes less time than with the previous method.

3.3.3 Genetic Operators

The flow chart of a GA is given in Figure 3.6. There are basically four genetic operators, selection, crossover, mutation and inversion.

Selection

The aim of the selection procedure is to reproduce more individuals whose fitness values are higher than those whose fitness values are lower. The selection procedure has a significant influence on driving the search towards a promising area and finding good solutions in a short time. However, the diversity of the population must be maintained to avoid premature convergence and to reach the global optimal solution.

Crossover

This operation is used to create two new individuals (children) from two existing individuals (parents) picked from the current population by the selection operation. Some common crossover operations are one-point crossover, two-point crossover and cycle crossover. One-point crossover is the simplest crossover operation. Two individuals are randomly selected as parents from the pool of individuals formed by the selection procedure and cut at a randomly selected point. The tails, which are the parts after the cutting point, are swapped and two new individuals (children) are produced.

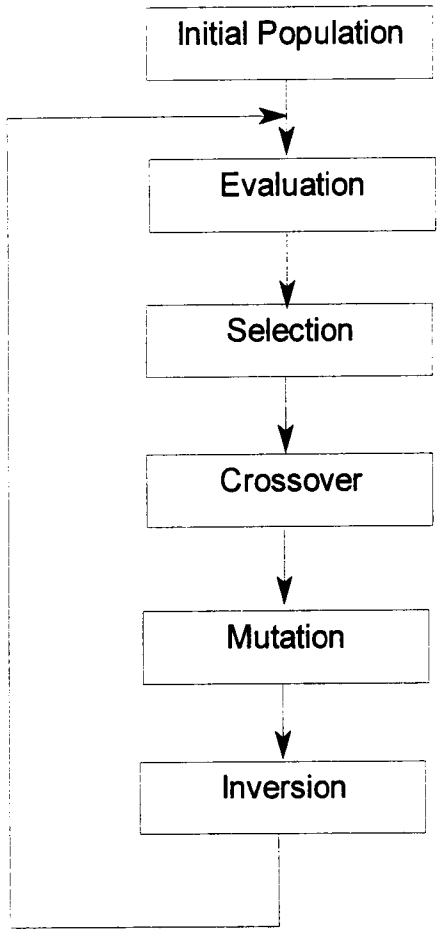


Figure 3.6: Flow chart of a GA.

Parent 1	**100|010011110**
Parent 2	**001|011000110**
Child 1	**100|011000110**
Child 2	**001|010011110**

Mutation

In this procedure, all individuals in the population are checked bit by bit and the bit values are randomly reversed according to a specified rate. The mutation operator forces the algorithm to search new areas. Eventually, it helps the GA avoid premature convergence and find the global optimal solution.

Old string	**1100|0|1011101**
New string	**1100|1|1011101**

Inversion

This procedure operates on one individual at a time. Two points are randomly selected from an individual and the part of the string between those two points is reversed.

Old string	**10|1100|11101**
New string	**10|0011|11101**

Important Parameters

Important parameters of a GA include population size, crossover rate, and mutation rate and inversion rate. A large population size means the simultaneous handling of many solutions and increases the computation time per iteration; however

since many samples from the search space are used, the probability of convergence to a global optimal solution is higher than when using a small population size. The crossover rate determines the frequency of the crossover operation. It is useful at the start of optimization to discover a promising region. A low crossover frequency decreases the speed of convergence to such an area. If the frequency is too high, it leads to saturation around one solution. The mutation operation is controlled by the mutation rate. A high mutation rate introduces high diversity in the population and might cause instability. On the other hand, it is usually very difficult for a GA to find a global optimal solution with too low a mutation rate.

Fitness Function

The fitness evaluation function acts as an interface between the GA and the optimization problem. Fitness functions might be complex or simple depending on the optimization problem. Where a mathematical equation cannot be formulated for this task, a rule-based procedure can be constructed for use as a fitness function or in some cases both can be combined. Where some constraints are very important and cannot be violated, the solutions that do so can be eliminated in advance by appropriately designing the representation scheme. Alternatively, they can be given low probabilities by using special penalty functions.

3.4 Fuzzy Logic and Fuzzy Reasoning

Although fuzzy logic has been described and examined for over 30 years, it has only recently gained popularity. Most of the attention in fuzzy logic has been in the area of control engineering, brought on by the fuzzy logic products developed in Japan.

3.4.1 Fuzzy Set Theory

Fuzzy set theory may be considered an extension of classical set theory. While classical set theory is about "crisp" sets with sharp boundaries, fuzzy set theory is concerned with "fuzzy" sets whose boundaries are "gray". In classical set theory, an element u can either belong or not belong to a set A, i.e. the degree to which element u belongs to set A is either 1 or 0. However, in fuzzy set theory, the degree of belonging of an element u to a fuzzy set A is a real number between 0 and 1. This is denoted by $\mu_A(u)$, the degree of membership of u in A [33-34]. Figure 3.7 illustrate the fuzzy sets for "high", "low", and "around".

3.4.2 Basic Operations on Fuzzy Sets

Fuzzy sets are defined by membership functions. Therefore, set operations are usually defined in terms of membership functions. The most commonly adopted definitions are those used by Zadeh [33]. The basic operations are

Intersection

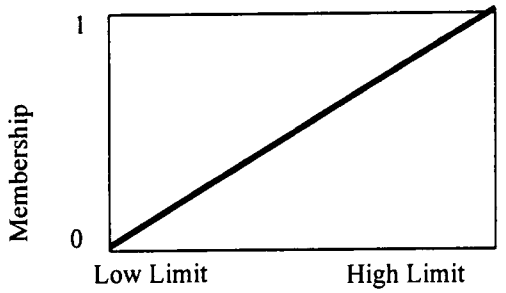
$$A \cap B = \min(\mu_A[x], \mu_B[y]) \qquad (3.14)$$

Union

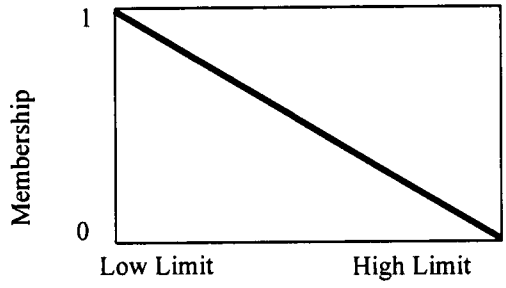
$$A \cup B = \max(\mu_A[x], \mu_B[y]) \qquad (3.15)$$

Complement

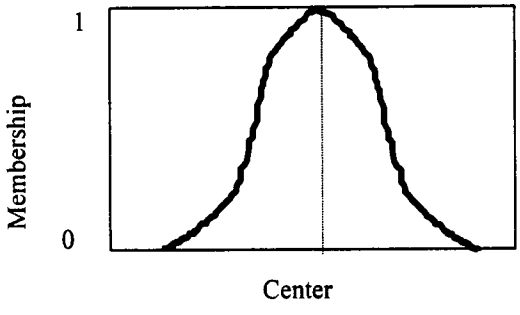
$$\widetilde{A} = 1 - \mu_A[x] \qquad (3.16)$$



(a)



(b)



(c)

Figure 3.7: Fuzzy sets. (a) "high" fuzzy set, (b) "low" fuzzy set, (c) "around" fuzzy set.

Since fuzzy sets are not crisply partitioned in the same sense as Boolean sets, these operations are applied at the truth membership level.

3.4.3 Fuzzy Relations and Linguistic Variables

A fuzzy system consists of a set of rules called "fuzzy rules". A simple fuzzy rule is of the following form:

"IF A_i THEN B_i"

where the antecedent A_i and the consequent B_i are linguistic variables. Example of linguistic variables is high, low, long, and short. A linguistic variable also carries with it the concept of fuzzy set qualifiers that are often called "hedges". These "hedges" change the shape of fuzzy sets in predictable ways and function in the same fashion as adverbs and adjectives. An example of "hedges" is very, extremely, about, around, close to, etc. A linguistic variable encapsulates the properties of approximate or imprecise concepts in a systematic and computationally useful way. It reduces the apparent complexity of describing a system by matching a semantic tag to the underlying concept.

3.4.4 Fuzzy Reasoning

Unlike conventional expert systems where statements are executed serially, the principal reasoning protocol behind fuzzy logic is a parallel-processing paradigm. The root mechanism in a fuzzy model is the proposition. These are statements of relationships between model variables and one or more fuzzy regions. A series of conditional and unconditional fuzzy associations or propositions is evaluated for its degree of truth and all those that have some truth contribute to the final output state of the solution variable set. The functional link between the degree of truth in related fuzzy regions is called the

method of implication. The functional link between fuzzy regions and the expected value of a set point is called the method of defuzzification. Taken together these constitute the approximate reasoning as shown in Figure 3.8 [36,37].

The benefits of fuzzy system over conventional expert system is listed as

- The ability to model highly complex or nonlinear problems,
- The ability to encode knowledge directly in a form that is very close to the way experts themselves think about the decision process,
- Improved handling of uncertainty and possibilities,
- Parallel processing of information.

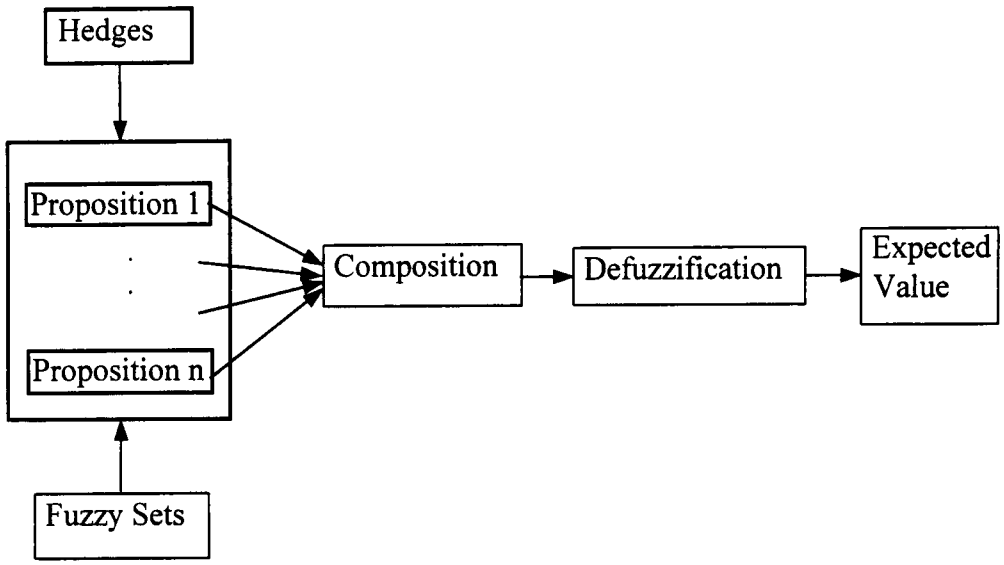


Figure 3.8: Fuzzy approximate reasoning.

CHAPTER 4

DESIGN OF THE NEW INSTRUMENT

As reviewed in the previous section, there is no integrated system to measure wool fiber properties. Some instruments are based on latest technology such as OFDA but the others still use 50's and 60's technology or older. In the cotton industry, both High Volume Instrument (HVI) and Advanced Fiber Information System (AFIS) are integrated systems to measure multiple cotton fiber properties such as length, fineness and trash content [38]. AFIS use the advanced Electro-optics technology to measure single fiber length and fineness. It also established a reference method for nep measurement and achieved great success in cotton textile industry [39]. AFIS length and diameter are based on single fiber measurement. Technically it is a better approach than those staple diagram based instrument (AL-Meter) or fibrogram based instrument (HVI). The limitation of the AFIS is that it can only measure fibers shorter than 50 mm. The purpose of this research project is to develop an integrated fiber information system for wool top properties based on advanced technology in digital signal processing, digital image processing and pattern recognition.

4.1 Review of AFIS Design

The Advanced Fiber Information System (AFIS) manufactured by Zellweger Uster Inc. was developed to measure cotton and short staple fiber properties. A general schematic of the system is shown in Figure 4.1. An aeromechanical system (Fiber

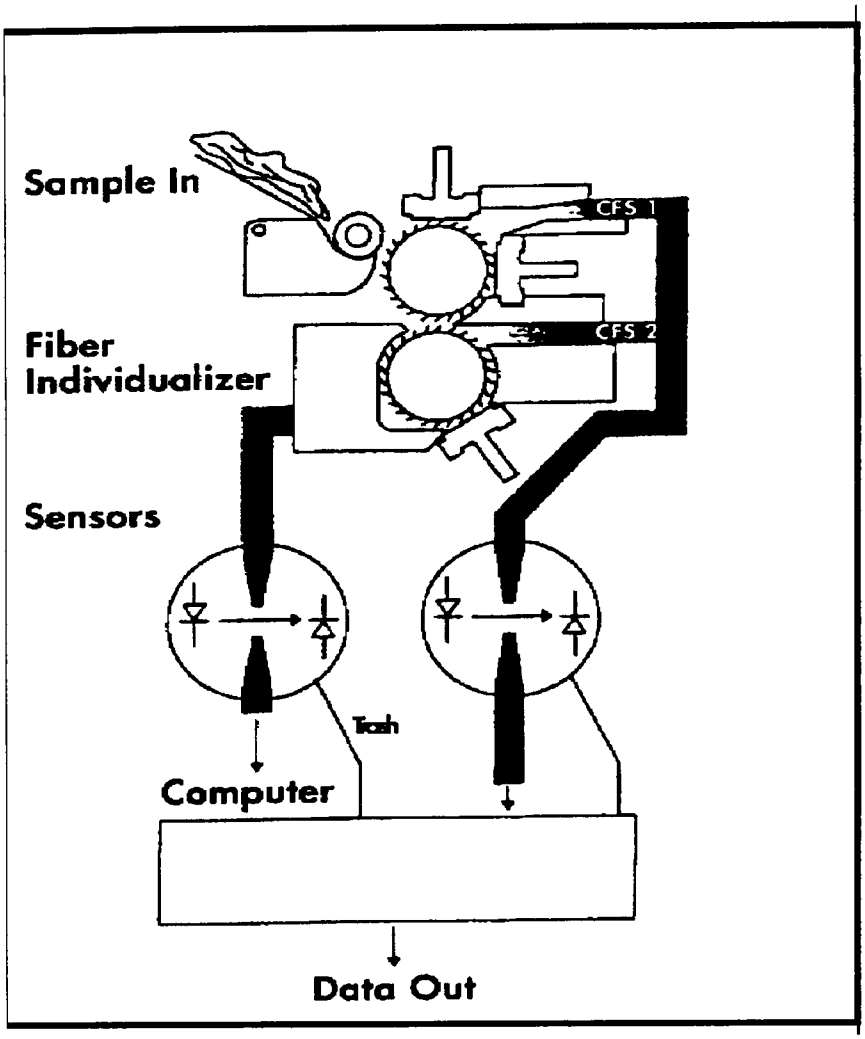


Figure 4.1: General Schematic of AFIS

Individualizer is used to separates the sample into three main components: lint, trash and dust. The foundation of the sample preparation device is the carding unit. The mini-card separates tufts into individual fibers and trash. Using gravimetric difference, the fibers and trash are separated and feed into different channels. The lint channel contains fibers and neps. The cleaned lint follows a pathway through a special acceleration nozzle and successive sensors for fiber length and diameter distribution and other measurements that require fiber individualization. The fibers are straightened or de-looped by the accelerating air stream before they were measured by the Electro-optics sensor. The trash channel contains trash, dust and very large seed coats. The trash size distribution was measured by another set of sensors. AFIS system is successful in measuring cotton fiber and short-staple man-made fibers. However, it can not measure wool and long-staple fibers because of the limitation of the sample preparation device, specifically, the carding process is too strong which will break fibers and the accelerating nozzle is not suitable to straighten and de-loop fibers as long as 300 mm.

4.2 Design of the New Instrument

Drafting is a method used in textile industry to reduce the linear density of the fiber strand. Using drafting, the slivers are drafted into roving and yarns. Similarly, it may be possible to draft slivers into individual fibers assuming the twisting is not used and the drafting ratio is high enough. Figure 4.2 illustrated the schematic of the new sample preparation device. There are two draft zones. The first drafting unit draw the

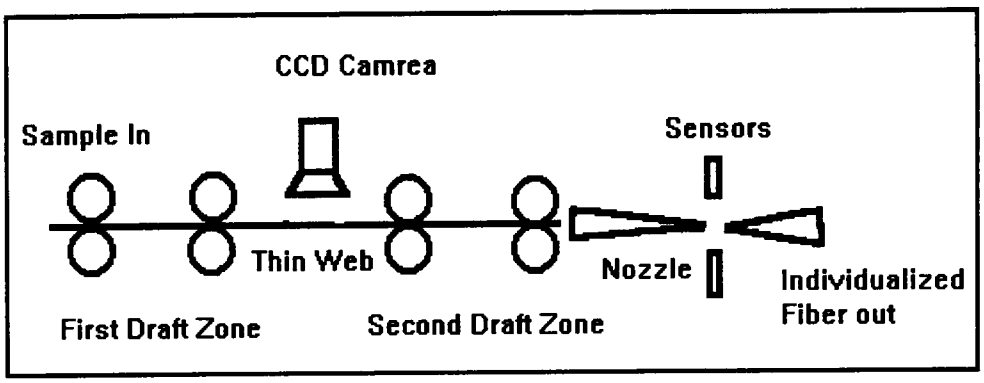


Figure 4.2: General Schematic of the New Instrument.

wool top into a thin web where neps, vegetable matter and dark-fibers can be measured using a CCD camera and a special designed illumination cylinder. The second drafting unit individualize the fibers by means of a very high drafting ratio. Individualized fibers were feed into an accelerating nozzle where single fibers were measured by several Electro-optics sensors for length and diameter and the fiber bundles were rejected by a waveform recognizer. There are many advantages of the new sample preparation device over AFIS. Because drafting will straighten the fibers, there will be less loop fibers than AFIS. The drafting process is gentler than carding process that will result in less fiber damage. By means of CCD camera, dark fibers can be detected on thin web and those fibers can not be separated using AFIS aeromechanical device.

4.2.1 Design of Sample Preparation Device

The sample preparation device has two drafting zones. The rollers and aprons are driven by stepper motors for better control of speed. The compressed air is used to control the pressure on rollers and aprons.

The Basic Mechanism of Drafting

Drafting is the process of elongating a strand of fibers, with the intentions of orienting the fibers in the direction of the strand and reducing its linear density [42]. The terms 'drafting' and 'drawing' are used interchangeably. In a roller-drafting system, the strand is passed through a series of sets of rollers, each successive set rotating at a surface velocity greater than that of the previous set. Each set of rollers grips the strand. Weighting by dead weights, springs, pneumatic-pressure systems, etc., is used to press the rollers together and to prevent slippage between the fiber and the rollers. Each two

sets of rollers adjacently placed from a drafting zone. If the linear velocity of the material in the back set is *u*, and the linear velocity of the material in the faster front set is *v*, the mechanical draft ratio is *v/u*. The actual draft ratio may not be the same as the mechanical draft ratio if the material slips at either set of rollers. A drafting system with x sets of rollers has no more than (x-1) drafting zones. If, for example, the draft ratios in the separate zones are D_1, D_2, and D_3, respectively, the total draft in the system is $D_1xD_2xD_3$. In practice, the last draft zone through which the strand passes in a system has the highest draft ratio and is called the main draft zone. In order to control fiber better in a draft zone, aprons may be used in main draft zone. Figure 4.3 illustrated the drafting unit used in sample preparation device.

Important Parameters of the Sample Preparation device

The sample preparation device should produce uniform thin webs for defect detection at the first measuring zone (output of the first drafting unit) and uniformly individualize the fibers for length and diameter measurement at the second measuring zone (output of the second drafting unit) without fiber damage. Therefore, the important parameters are drafting ratio, output speed, and pressure on apron and distance between the roller nips.

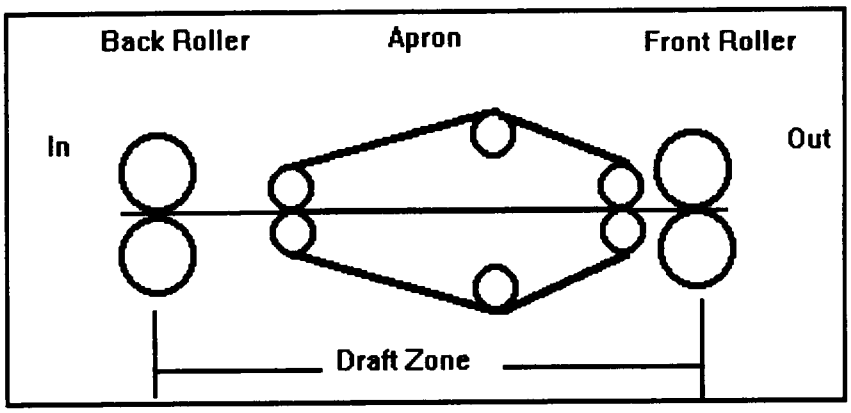


Figure 4.3: Drafting Unit Used in Sample Preparation Device.

(1) Distance between the Roller Nips

The distance between roller nips should be equal to at least the maximum fiber length or else fiber breakage will occur. In practice, additional clearance is required.

(2) Drafting Ratio

In order to produce uniform web at the first stage and individualize the fibers at the second stage, the drafting ratio should be properly setup. The first drafting unit should draw the top into a very thin web but maintain the web continuity. The range of drafting ratio will be around 10 to 30 depend on the input top weight. The second drafting unit should individualize the fibers. If the maximum fiber length is 300 mm and the minimum resolution of separation is 1 mm, the minimum drafting ratio is 300. The process of individualization can be explained as the follows.

If fiber A reaches the nip of the front roller and fiber B is hold by the nip of the apron, fiber A will travel at the front roller speed v1 and fiber B will travel at the apron speed v2. If v1/v2 > maximum fiber length L, fiber A and B will be separated as shown in Figure 4.4.

If fiber A and B reach the front roller at the same time and having the same length, they will accelerate to v1 at the same time and wont be separated. Waveforms from photo-detector will have both bundle fibers and single fibers and the signal processing algorithm will reject the bundle fiber waveforms.

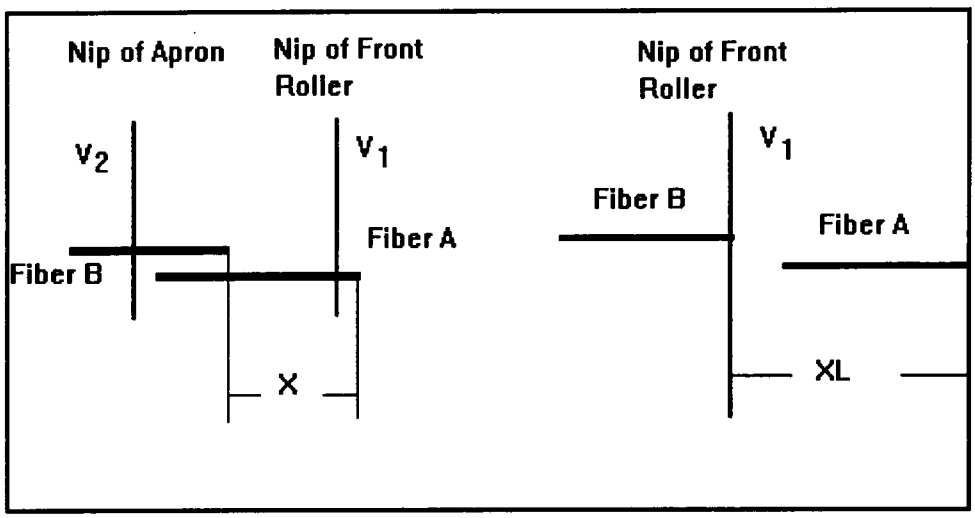


Figure 4.4: Principle of Individualization by Drafting.

(3) Pressure

The fibers passing through the nip of a pair of rollers should be held firmly so that they have no motion other than that dictated by the rollers. The pressure on apron should be setup properly. The apron should hold the fibers that have not reach the front roller and allow slippage for the fibers who have griped by the front roller. The appropriate pressure will be determined by the experiment.

(4) Output Speed

The output speed should meet the requirement of minimum throughput of the instrument and match the speed of gas velocity of the nozzle. If output speed is higher than gas velocity in the nozzle, loop fibers will be generated.

4.2.2 Design of Defects Detector

Illumination

The defect detector comprises an illumination cylinder and a CCD camera to detect colored fibers, vegetable matter and neps. Colored fibers are difficult to see in sliver unless non-colored fibers are rendered "invisible" in some way. One approach is to use balanced illumination whereby a web of sliver is illuminated equally from above and below. The balanced illumination allows colored fibers to be readily identified and removed for later analysis [8]. To completely suppress the normal fibers, cavity illumination might be used as described by P.W.Chudleigh of CSIRO wool technology [41]. Suppose there are diffuse sources to form a cavity with a luminous surface of arbitrary shape that completely encloses the fiber web as shown in Figure 4.5. Light

emitted from all points on the cavity walls is assumed to be uniformly diffuse and unaffected by the presence of a small viewing aperture in the roof of the cavity. Under these idealized conditions, the light intensity at all points within the cavity is uniform and isotropic, then, the images formed by transparent fibers with circular cross section are completely suppressed. In practice, an integrating cylinder as shown in Figure 4.6 can approximate the cavity. Figure 4.7 illustrated the result of cavity illumination. The result is quite impressive.

Image Acquisition System

The image acquisition system includes a Pulnix monochrome CCD camera, a 9'' Panasonic TV monitor, a Pentium 133 PC, a Dipix XPG 1000 DSP frame grabber and a strobbing control circuit with LED as light source as shown in Figure 4.8. Dipix XPG 1000 frame grabber has a TI C40 DSP processor, so that the image processing and recognition task can be done using DSP while host PC can do other tasks such as display, motor control etc.

4.2.3 Design of Single Fiber Detector

AFIS single fiber detector and data acquisition system was adapted to the new instrument with minor modifications.

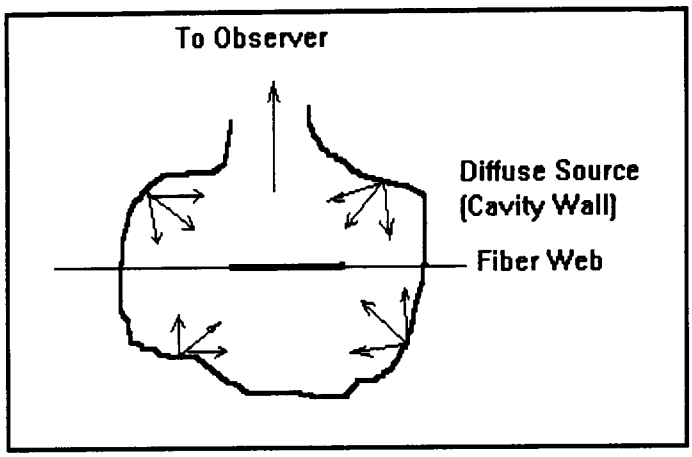


Figure 4.5: Cavity Illumination.

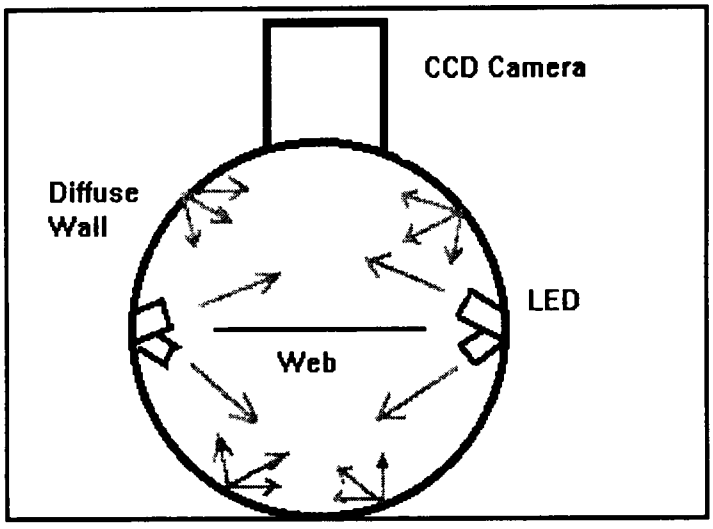


Figure 4.6: Integrating Cylinder.

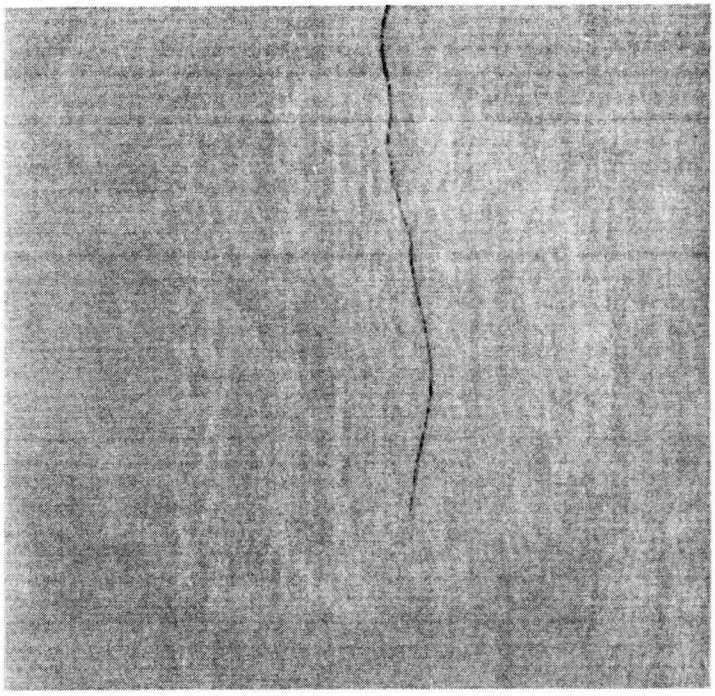


Figure 4.7: Image of One Dark Fiber among Many Normal Fibers by Integrating Cylinder.

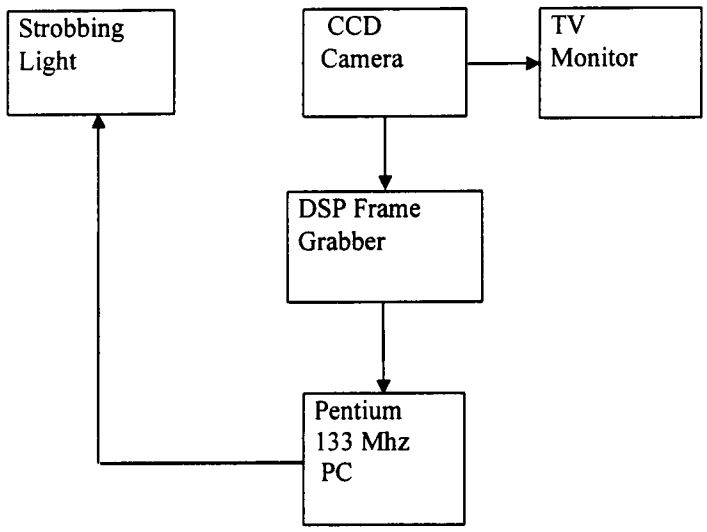


Figure 4.8: Image acquisition system.

Nozzle and Detectors

The single fiber detector comprise a accelerating nozzle, two pairs of LED and photo detectors, and a signal conditioner to detect individualized fibers for length and diameter measurement as shown in Figure 4.9. The reason for use two pairs of detector is to measure the fiber flying speed. This single fiber detector is a modified version of AFIS single fiber detector. The detection principle is the same as AFIS but the signal processing is different using the advanced technology in digital signal processing (DSP). The details will be discussed in next chapter.

Data Acquisition System

The data acquisition system include a signal conditioner, a LED servo, and a Keithley data acquisition board as shown in Figure 4.10.

4.2.4 Software Development

The waveform analysis software, image processing software and pattern recognition software were developed using C language and some of the user interface software were developed in Visual Basic.

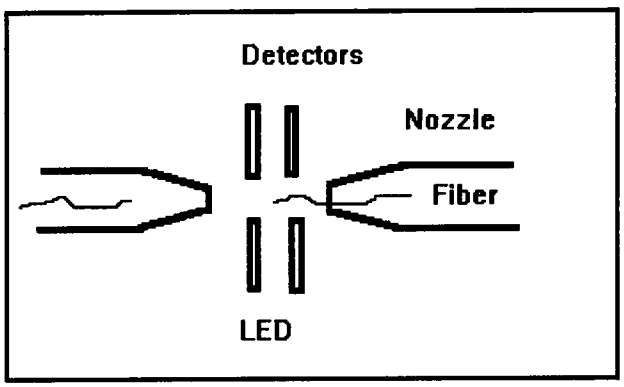


Figure 4.9: Single Fiber Detector.

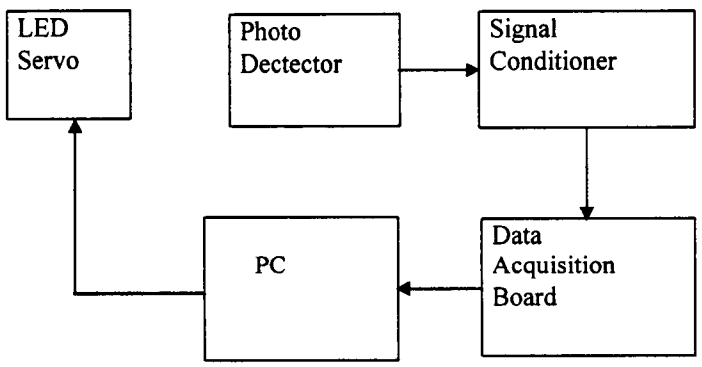


Figure 4.10: Data acquisition system.

CHAPTER 5

WOOL TOP LENGTH AND DIAMETER MEASUREMENT

5.1 Length and Diameter Measurement from Normal Single Fiber Waveform

Most of the fibers passing through the sensors are single fibers but there are some bundle fibers and loop fibers. The digital signal-processing task is to reject the bundle and loop fibers. The length and diameter measurement will be based on single fiber waveforms. The assumption is that the rejection of bundle and loop fibers won't cause bias in measurement results.

5.1.1 Length Models from the Waveform

A typical signal from electro-optics sensor is plotted in Figure 5.1. There are two waveforms correspond to the two of the photo-detectors. The time of flying (T) for a single fiber will depend on fiber length and fiber mass (diameter and linear density). The longer the length (L), the longer the time of flying will be. Also, the heavier the fiber, the longer the time of flying. In figure 5.1, d is the distance between the two sensors, T_b is the flying time of the leading end of the fiber from the first sensor to the second sensor. T_e is the flying time between the two sensors for the trailing end of the fiber. For longer fibers, T_b will be expected to be larger than those from the shorter fibers because the fiber mass is heavier at the beginning of the acceleration. T_b vs L is plotted in Figure 5.2 (a).

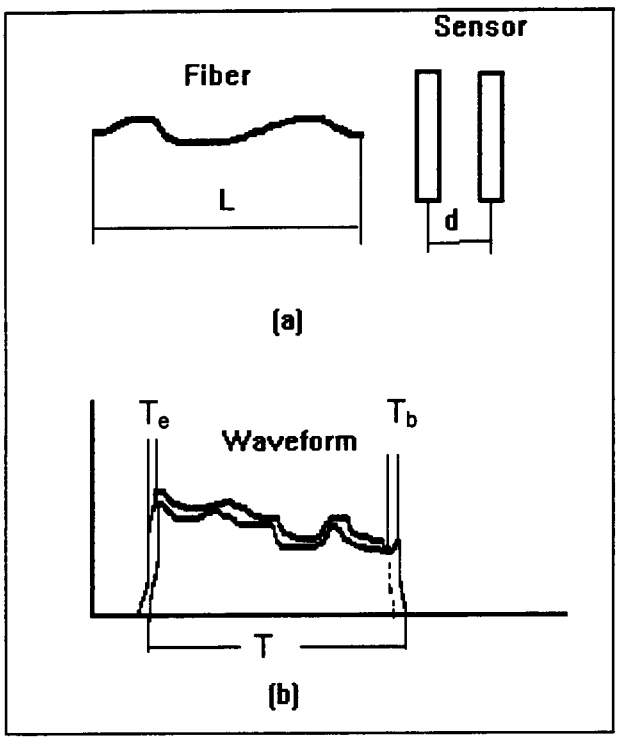
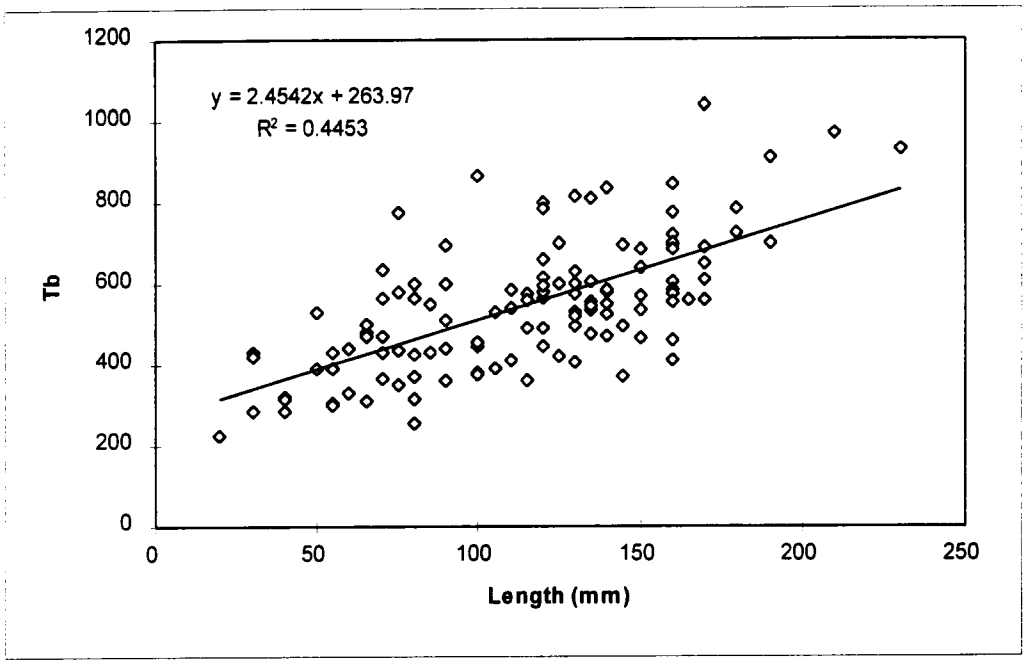
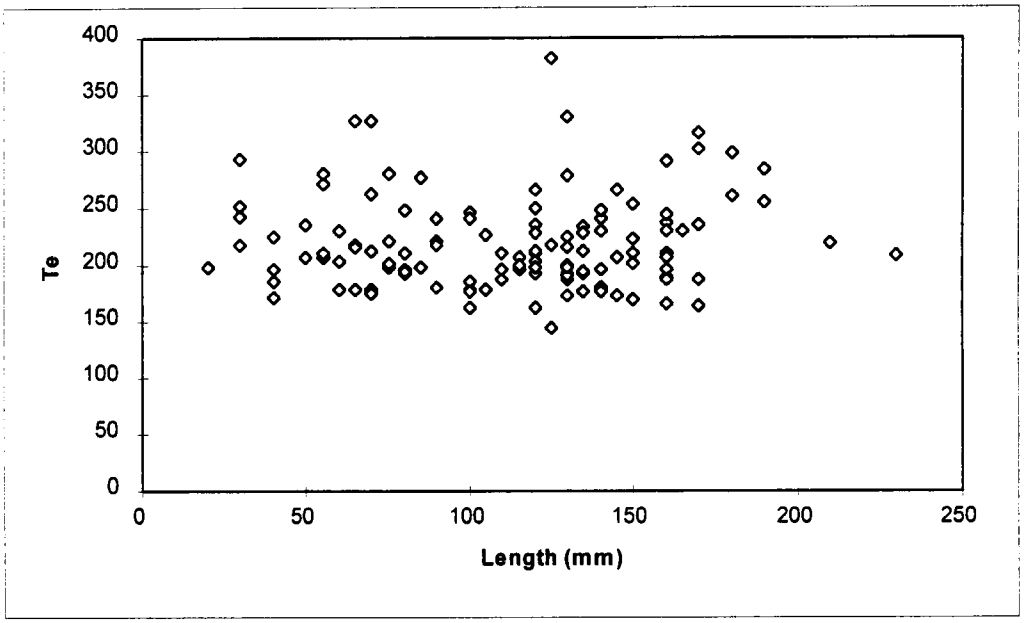


Figure 5.1: (a) Fiber and sensors. (b) Fiber waveform from the two sensors.



(a)



(b)

Figure 5.2: T_b, T_e and L. (a) T_b vs L, (b) T_e vs L.

Although correlation is not high, the relationship between T_b and L is still hold. T_e is not correlated with length because the scatter as shown in Figure 5.2 (b).

Physical Model

Based on the assumptions, physical model can be developed for approximation. The model assumes that the fiber traveling between the two sensors in a constant acceleration [42]. From physics, we know that velocity, acceleration and distance has the following relationship

$$v = v_0 + at \qquad (5.1)$$

$$x = v_0 t + \frac{1}{2} a t^2 \qquad (5.2)$$

$$v^2 = v_0^2 + 2ax \qquad (5.3)$$

where v is the velocity, v_0 is the initial velocity, t is the time and x is the distance traveled. In our case,

$$v_0 = \frac{d}{T_b} \qquad (5.4)$$

$$v = \frac{d}{T_e} \qquad (5.5)$$

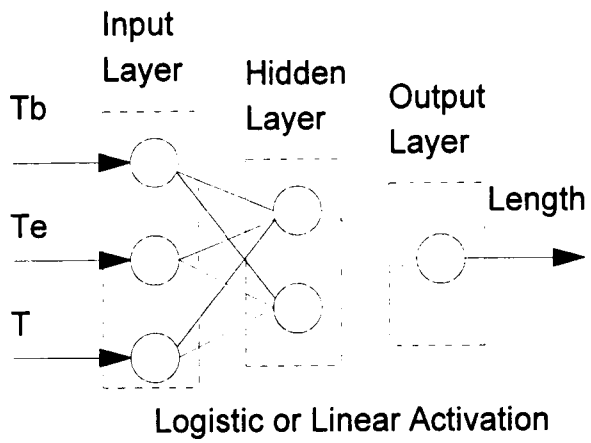
where d is the distance between the two sensors. Substitute v_0 and v to equation (5.1) to (5.3), we get the following equation for length measurement

$$L = \frac{1}{2} dT \frac{T_b + T_e}{T_b T_e} \qquad (5.6)$$

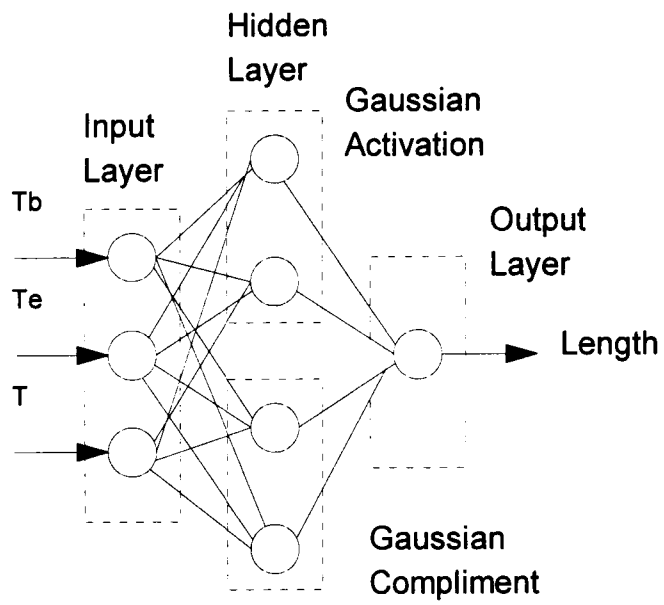
where L is the fiber length, T is the time of flying from the first waveform; d is the distance between the two sensors.

Empirical Model

Because fiber mass is not uniform along the length, and crimp will affect the air drag, etc, fiber movement in air stream is very complicated. With so many unknown influences, empirical model can be tried. As discussed in Chapter 3, neural networks is a black-box approach to solve input - output relations. A three-layer MLP network is tried to develop length model with T_b, T_e and T as inputs and fiber length as output. Figure 5.3 illustrated the neural network configuration. Three empirical models were developed using three different network configurations. The first one use MLP with logistic function as activation function for all three layers; the second use linear function instead; the third configuration use two slabs in the hidden layer, one with Gaussian and another with Gaussian complement as activation function. The networks were trained with single fiber data from hand drop experiment. In training the MLP network, some parameters need to be determined which are important to the performance. These parameters include the number of hidden layers, the number of neurons in the hidden layer, learning rate and momentum coefficients. How many hidden layers are needed for a given problem? Hecht-Nielsen [19] has proven that a network with only one hidden layer can compute any arbitrary function of its inputs, therefore, one hidden layer will be used in developing empirical models. The hidden layer is a critical part in the network's learning phase. With appropriate number of hidden neurons, a MLP network is capable of realizing arbitrary



(a)



(b)

Figure 5.3: MLP configuration. (a) MLP with logistic or linear activation function, (b) MLP with 2 slabs in hidden layer, with Gaussian and Gaussian compliment activation function.

continuous functions defined on a hypercube [15]. With too few hidden neurons, the network is unable to create adequately complex decision boundaries. However, if there is a large number of hidden neurons, it is more difficult for the trained network to create a generalized mapping using the training data. The network will perform well on training data but fail on unseen data set. Some researchers have found that the number of hidden neurons depends on the number of input or output neurons. Kudrycki [15] predicted that the maximum number of hidden neurons for a single hidden layer should equal to output neuron x 3. Hecht-nielsen [19] showed those 2N+1 hidden neurons is an upper bound for a network with one hidden layer to compute an arbitrary function, where N is the number of network inputs. It is obvious that there is no general rule to select the optimal number of hidden nodes matching all the applications. This number is depends on the application and is selected based on the given problem. There are two approaches to arrive at a hidden layer structure. One approach is to start with no-hidden neuron, and add the hidden neurons gradually during training [14]. The other is to start with many hidden neurons in the network and remove unimportant ones from the network during training. In this project, the first approach is used to find the hidden neurons needed. The training algorithm is:

1. Partition the data set into training and testing set,
2. Initiate the MLP with one hidden neuron,
3. Training the MLP with the training set,
4. Evaluation the results with the testing set, if the error rate is within a tolerance or the error rate did not show significant improvement, terminate, else, add one neuron to the hidden layer and go to step 3.

Learning rate and momentum are also important parameters in training a MLP network. If there are a great deal of noise in the data set, a low learning rate (0.05 or 0.1) with a high momentum (0.5 or 0.6) is a good starting point. There are no firm rules on selecting these parameters and experience and trial and error are still the best way to know.

Evaluation of the models

In order to evaluate the models, a testing data set of 129 fibers was collected from four different wool samples with wide range of diameter and length using hand drop technique. Individual fibers were pull out from the sample and placed on a black board; the length were manually measured by a ruler and then the fibers were hand dropped into the nozzle one by one; the waveforms were recorded and analyzed by the models developed. The loop fibers were rejected by visual inspection. The results are plotted in Figure 5.4. Although all the models performed well with $R^2 > 0.9$, physical model with constant acceleration assumption achieved the best result. However, all the models from neural network show higher scatter in normal wool fiber and shorter fiber region (< 100mm). Within the MLP models, MLP with linear activation function (MLP_2) show better correlation than logistic function (MLP_1); MLP_3, which has two slabs in the hidden layer, show highest correlation but it is not as good as physical model in shorter

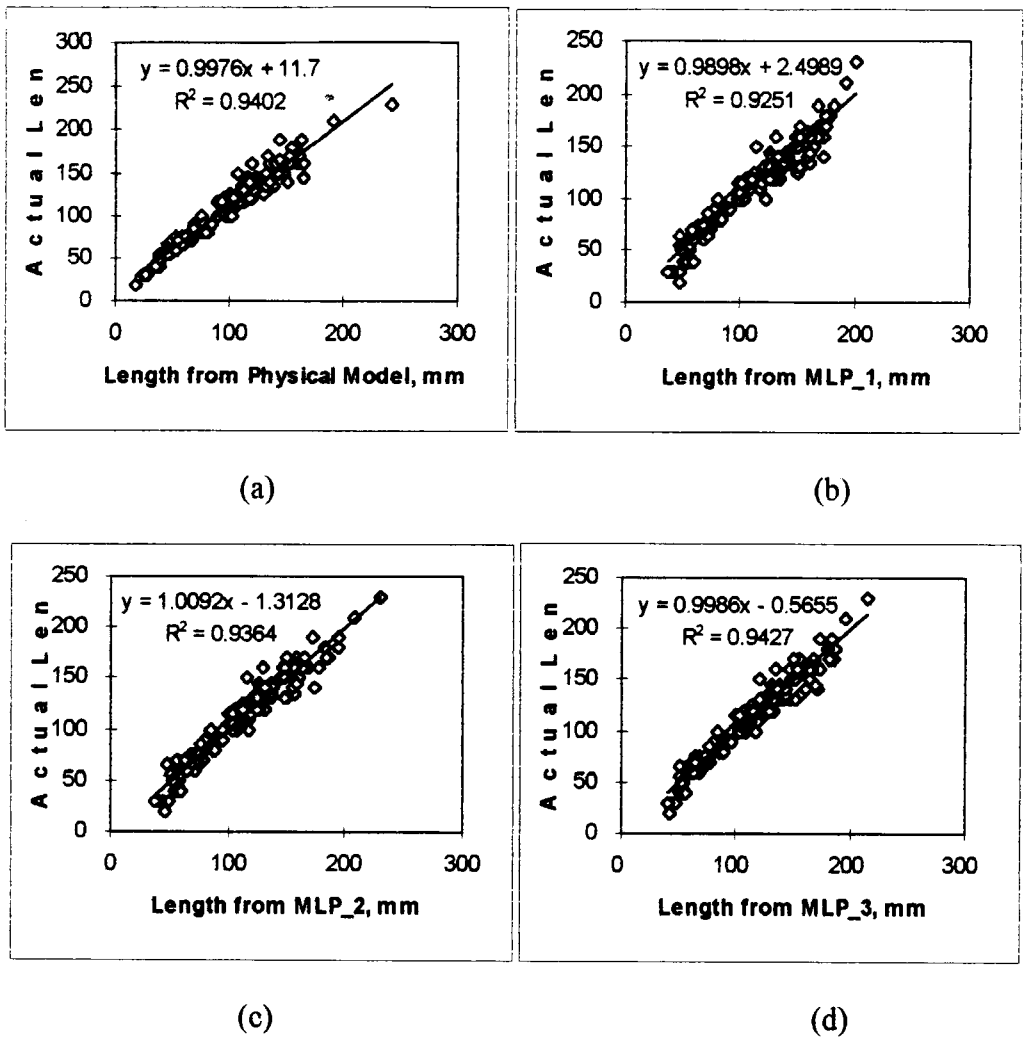


Figure 5.4: Results from physical and empirical models. (a) physical model, (b) MLP model with logistic activation function, (c) MLP model with linear activation function, (d) MLP model with two slabs in hidden layer.

fiber region. Figure 5.5 plots the length from MLP_3 vs. length from physical model. Correlation is high with $R^2 = 0.97$. Figure 5.6 illustrated the results from MLP_3 and physical model in comparison with the manual measurement. This experiment show that constant acceleration model gives a good approximation of fiber movement in nozzle. The results also show that the neural network learned the physical law from the experience in learning.

5.1.2 Diameter Measurement

The height of the waveform is proportional to the diameter of the fiber. Because the crimp will affect the waveform, the diameter might be measured at the minimum height of the waveform as shown in Figure 5.7.

5.2 Waveform Analysis and Feature Selection

Length and diameter measurements are based on fiber waveforms. Because the fiber individualizer can not individualize all fibers, the waveforms obtained from the sensor will be classified into single fiber waveforms and bundle / loop fiber waveforms. Figure 5.8 illustrated the typical waveforms. Figure 5.8 (a) and (b) are normal single fiber waveforms. Figure 5.8 (c) and (d) are single fiber waveforms with spikes but wont affect length measurement. Figure 5.8 (e) and (f) are loop fibers that should be rejected unless a de-looping algorithm is applied. Figure 5.8 (g) is either overlapping fiber or a short fiber parallel with a long fiber. Figure 5.8 (h) is a typical bundle fiber waveform. Fiber length measurement will be based on the length of the waveform, therefore, waveform (a), (b), (c) and (d) are measurable and (e), (f), (g) and (h) should be rejected. Fiber diameter

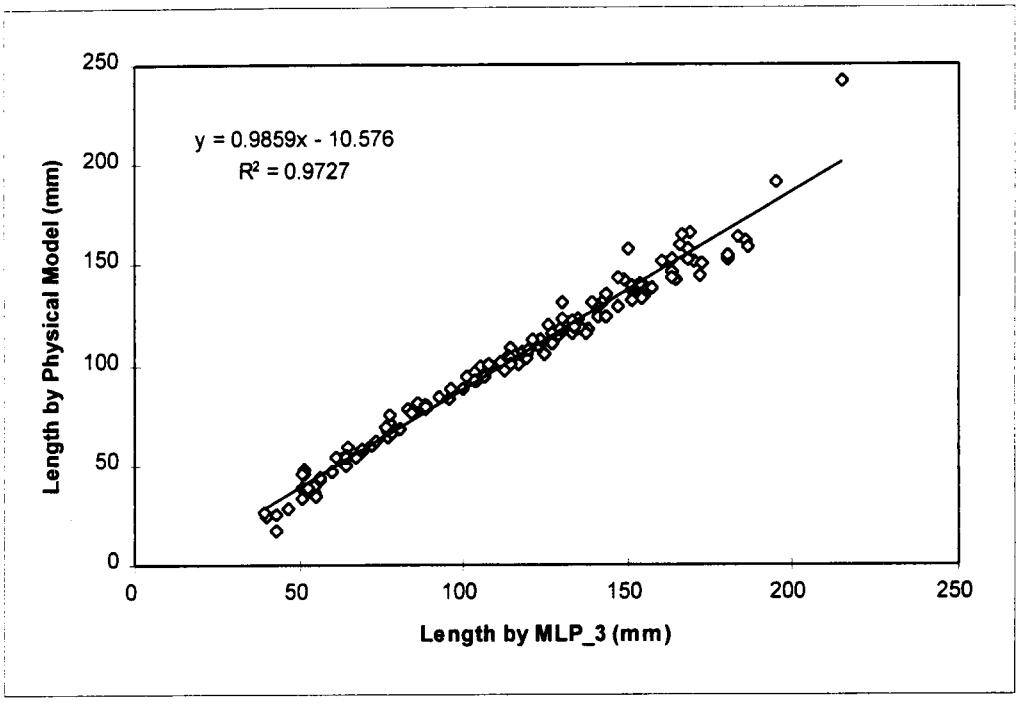


Figure 5.5: Length from physical model vs MLP_3 model.

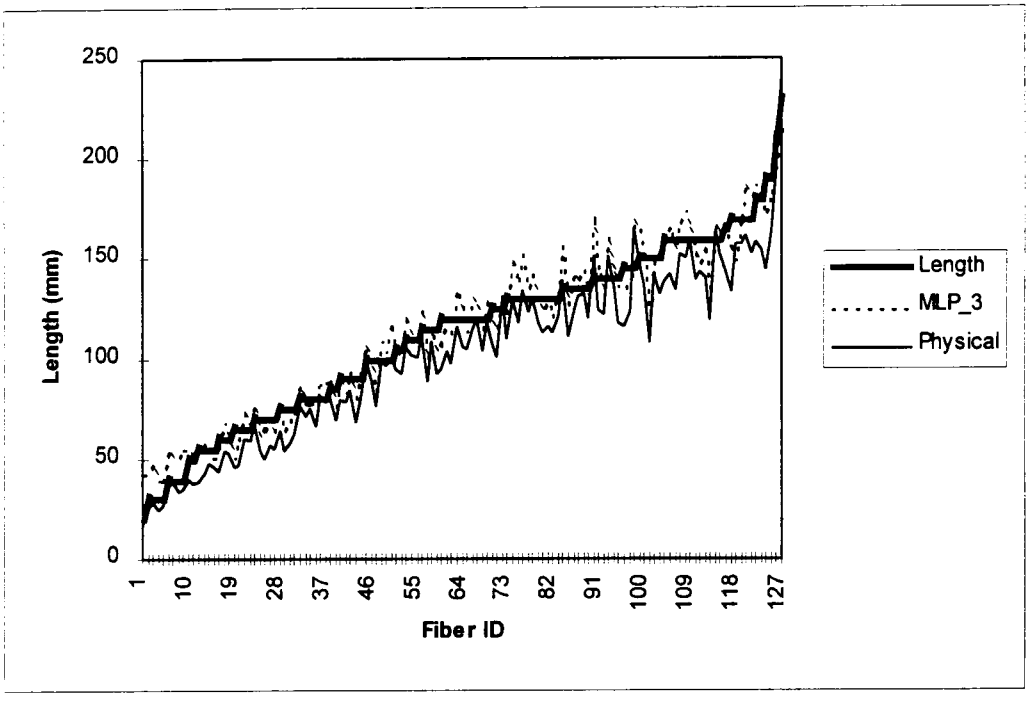


Figure 5.6: Results of length from manual measurement, physical model and neural network model.

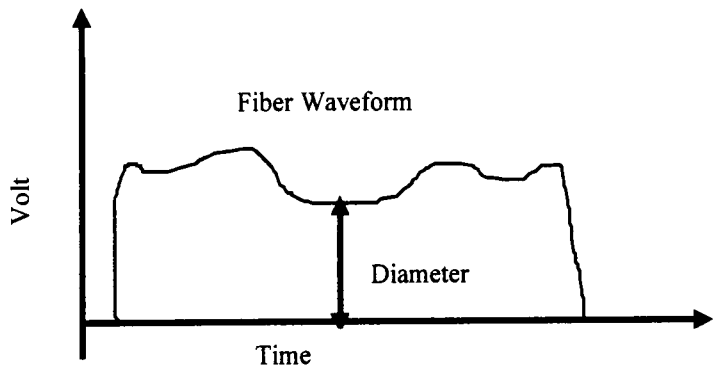


Figure 5.7: Diameter measurement from waveform.

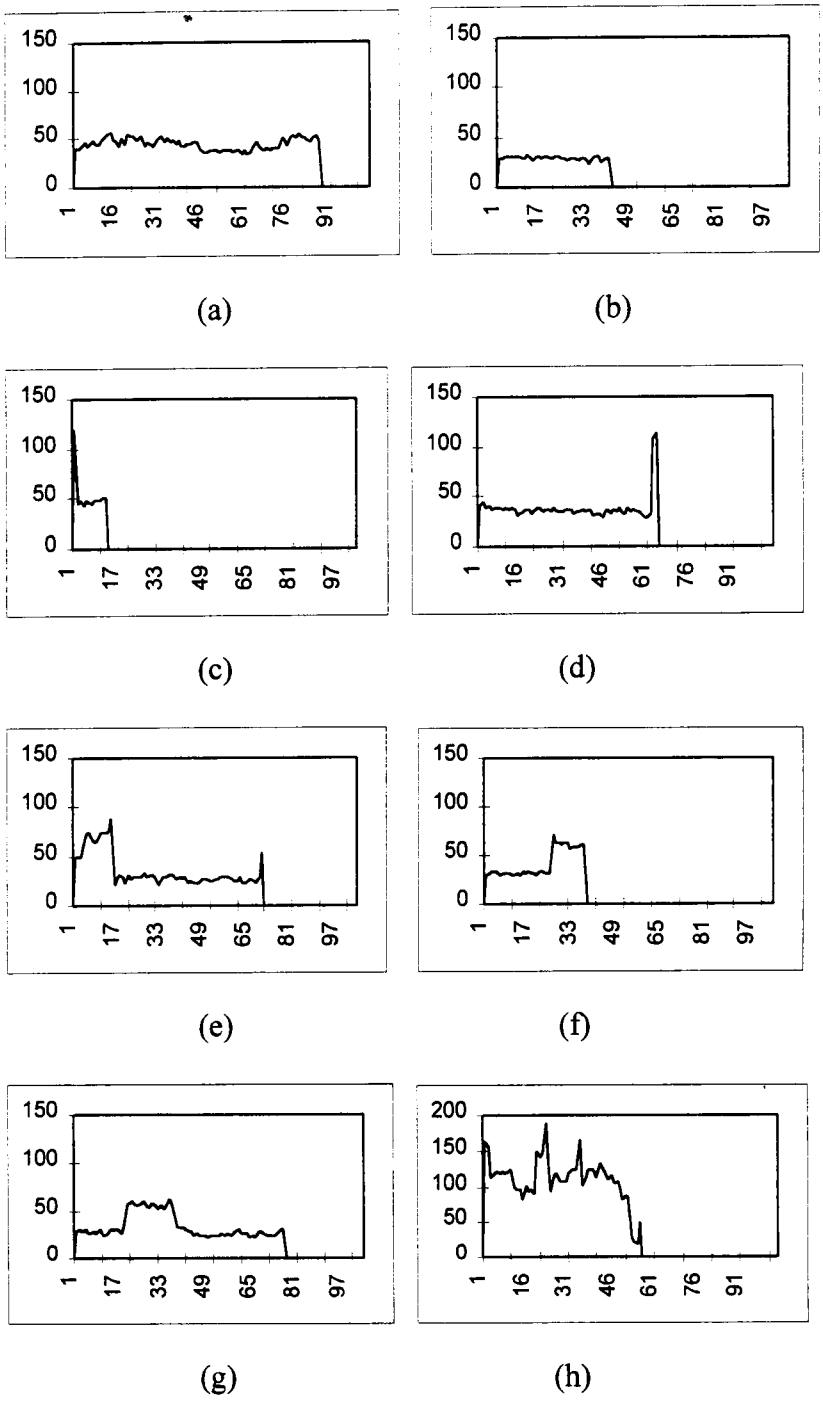


Figure 5.8: Typical Waveforms. (a), (b) normal single fiber waveforms, (c) single fiber waveform with left spike, (d) single fiber wavform with right spike, (e) left-loop fiber waveform, (f) right-loop fiber waveform, (g) overlap fiber waveform, (h) bundle fiber waveform.

measurement will be based on the height of the waveform. For loop fiber waveforms, diameter still can be obtained in non-loop regions, therefore, only waveform (d) should be rejected. As described above, the incoming waveforms will be classified into normal fibers, loop fibers and bundle fibers.

5.2.1 Feature Selection

Feature selection is the most important step in pattern recognition. Because this process is case dependent, there is no fixed rule on how to select the features. Some features are easy to perceive by human while some other features are not so apparent, usually they are obtained from transformation techniques. In this study, the feature set is selected directly from the waveform.

The features directly from waveform are

1. Shape Factor ---- rectangularity, (peak • length / area)
2. Vmax --- the peak of the waveform
3. Vmin --- the minimum voltage of the waveform
4. Vstart --- the voltage at the starting portion of the waveform
5. Vend --- the voltage at the ending portion of the waveform
6. Maximun Slope --- the maximum slope in the entire waveform
7. Vleft --- the mean voltage from Vstart to Maximum Slope
8. Vright --- the mean voltage from Maximum slope to Vend

Features 2 to 5 are illustrated in Figure 5.9. It is noticed that Vstart and Vend are not taken from the rising edge or falling edge, rather, they are taken at a distance to the two edges. The reason is to avoid the spikes region so that waveform (c) and (d) in Figure 5.8 can be classified as measurable class. Peak is related to bundle fiber waveforms, the higher the peak, and the more likely the bundle. AFIS use peak only to classify waveforms into single and bundle fiber waveforms. In fact, using peak only can not discriminate waveforms satisfactory. The overlap region in Figure 5.10 is possibly from loop fibers. The ratio of Vleft and Vright are related to loop fibers. If the ratio is close to two, possibly, it is a tail loop fiber. If the ratio is close to 0.5, it may be a head loop fiber. Shape factor is a measure of similarity of a normal single fiber waveform with 1.0 for a rectangular waveform. Because the normal single fiber waveform is not the ideal rectangular waveform, shape factor alone is not enough to classify the measurable and non-measurable class. Figure 5.11 illustrates the distribution of shape factor for the two classes. The overlap region is where the classification error occurs.

5.3 Waveform Recognition

5.3.1 Training and Testing Set

The training set has 296 waveforms selected from nine samples with wide range of length and diameter. Among the 296 waveforms, there are 179 normal single fiber waveforms, 51 loop fibers and 66 bundle fibers. Another 180 waveforms were selected for testing. There are 110 normal fibers, 33 loop fibers and 57 bundle fibers. These

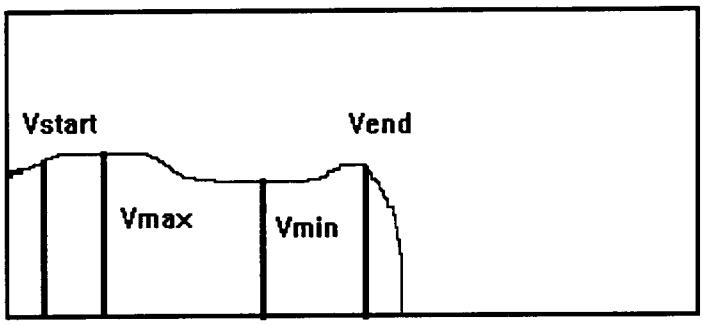


Figure 5.9: Features from waveform.

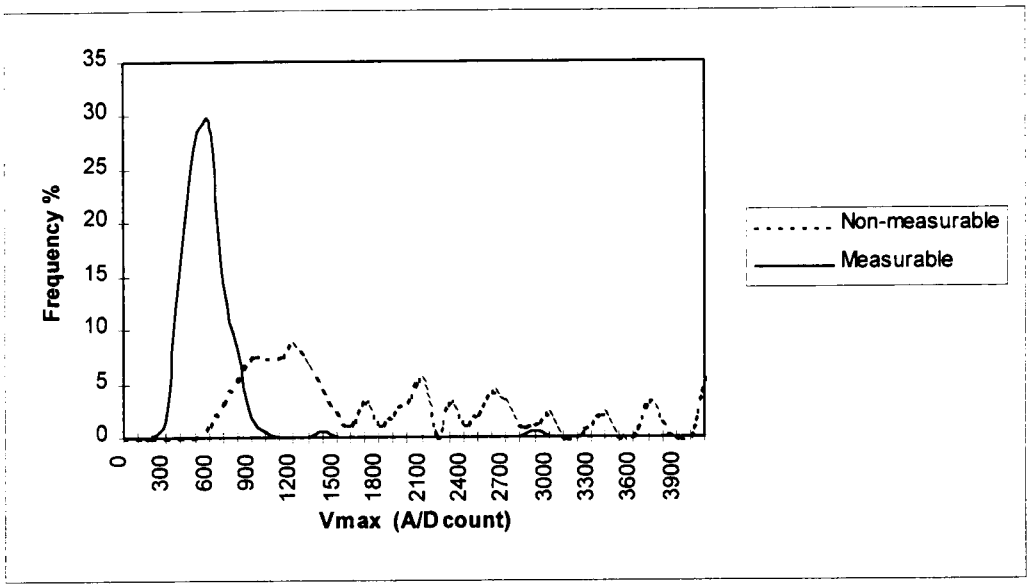


Figure 5.10: Peak voltage distribution.

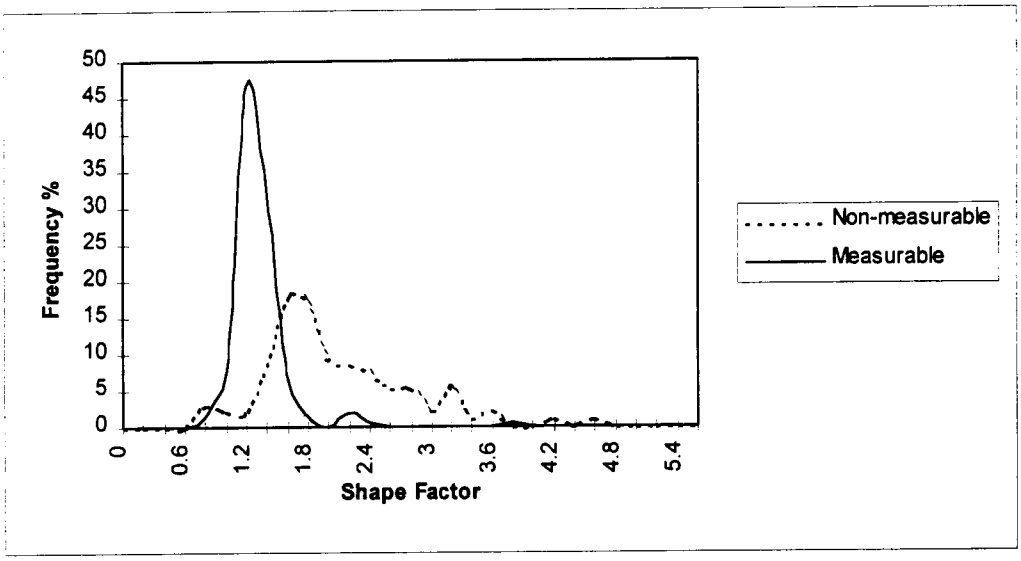


Figure 5.11: Shape factor distribution.

waveforms were visually classified into three categories. Because visual classification won't be consistent enough, there may have classification errors, especially for waveforms with spikes.

In order to select the best classifier for waveform classification, both neural network classifiers and rule-based classifiers were developed and evaluated using the feature set.

5.3.2 Waveform Recognition by Optimized Decision Tree

By analyzing the waveform, a decision tree can be constructed to classify waveforms into measurable and non-measurable class. Figure 5.12 shows the decision tree. T_1 to T_4 are decision thresholds those are determined by training. The selection of these thresholds and the combination of them are critical to total classification errors and need to be optimized. As described in Chapter 3, Genetic Algorithm is a new powerful technology to solve optimization problems especially in case where a fitness function can not be mathematically expressed or to solve combinational problems. Here, GA is applied to optimize the thresholds for the decision tree. The software procedure of the process is outlined below:

1. Create an initial population of individuals with a random number generator, each one of which can be interpreted as a group of selected thresholds,
2. Set up and train the decision tree with the thresholds selected by step 1,
3. Transfer the classification error to the fitness function to evaluate the fitness,

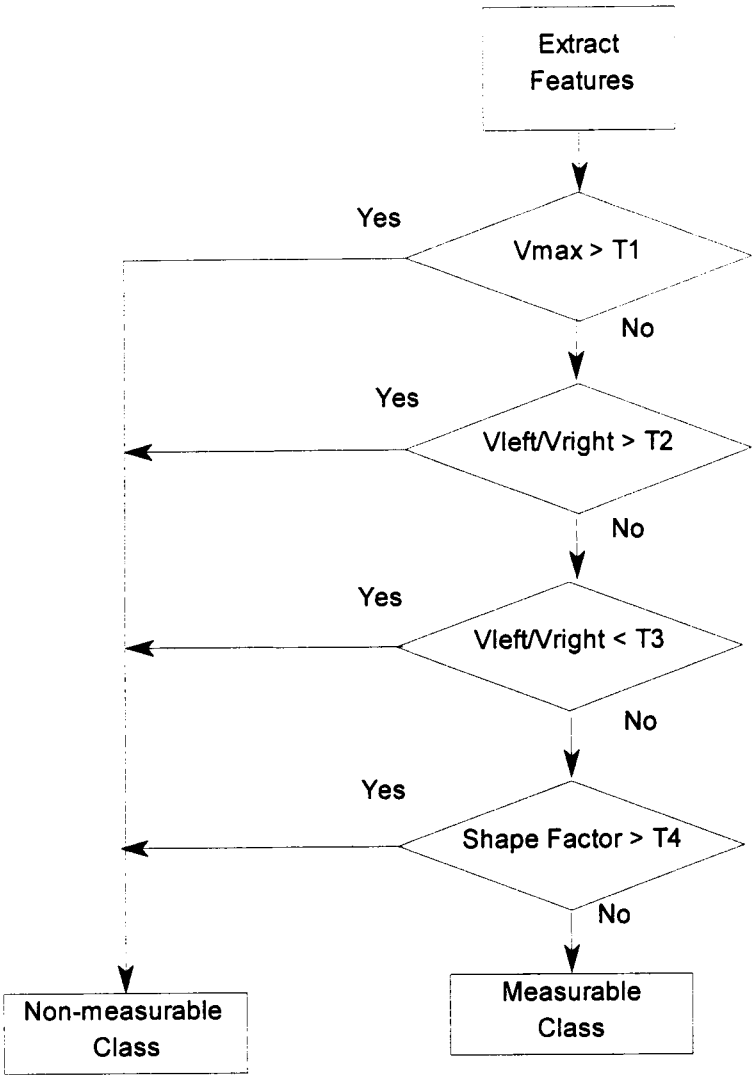


Figure 5.12: Flow chart of classification.

4. Perform the operation of genetic algorithms to create a new population of the individuals,
5. Repeat steps 2-4 till there is no further improvement in reducing classification error.

There are two parameters we should consider in implementing GA. These are crossover rate and mutation rate. The crossover rate is the probability that crossover will occur; it is chosen in a way so that recombination of potential strings (highly fitted chromosomes) increases without any disruption. Generally, the crossover probability lies in-between 0.6 to 0.9 [29, 32]. The mutation rate is the probability of mutation. Since mutation occurs occasionally, it is clear that the probability of performing mutation operation will be very low. Typically the value lies between 0.001 to 0.01 [29, 32]. Crossover rate of 0.9 and mutation rate of 0.01 was selected for finding the optimized thresholds.

The mechanism of the GA guarantees the convergence of the search to find an optimal group of thresholds that give superior performance with highest fitness, which in turn means the smallest training error. Table 5.1 shows the testing results. There are 12 total classification errors within 197 waveforms, which results in an error rate of 6.1 %. Four waveforms out of 65 non-measurable waveforms were classified as measurable class that results in a 6 % of false positive for measurable class. Eight waveforms out of 132 waveforms were classified as non-measurable class which results in an almost the same 6 % of false positive for non-measurable class.

Table 5.1: Decision tree classification results from testing set.

Class	Measurable	Non-measurable
Actual	132	65
Classified	128	69
True Positives	124	61
False Positives	4	8
True Positive Proportion	0.94	0.94
False Positive Proportion	0.06	0.06

5.3.3 Waveform Recognition by Probabilistic Neural Networks

PNN has a parameter, σ, a smoothing factor that applies to the probability density estimates (eq.3.13). σ is crucial to competent performance, yet there is no universal, mathematically rigorous method for choosing the best value. The optimal value of σ for every problem is different. It may be on the order of 1, or it may be on the order of 0.001. Figure 5.13 illustrates the classification error at three σ values from the testing set. σ too low or too high will both result in higher classification error. In order to find the best σ to classify waveforms, Genetic Algorithm was applied to minimize the classification error with σ as a chromosome and the total classification error as fitness function. Table 5.2 lists the result from optimization of σ using GA. The optimized σ is found at σ=0.068 after 36 generations. Within 197 waveforms, there are 10 waveforms were classified wrong which resulted in 5.1 % total error rate which is lower than rule-based classifier (6.1%). Looking at the details, classification for measurable class is satisfactory. There are 132 waveforms and only 4 of them were classified wrong. For non-measurable class, there are 6 miss-classification in 65 waveforms. The error rate is about 9 % that are not low enough compared to the 6% from rule-based classifier.

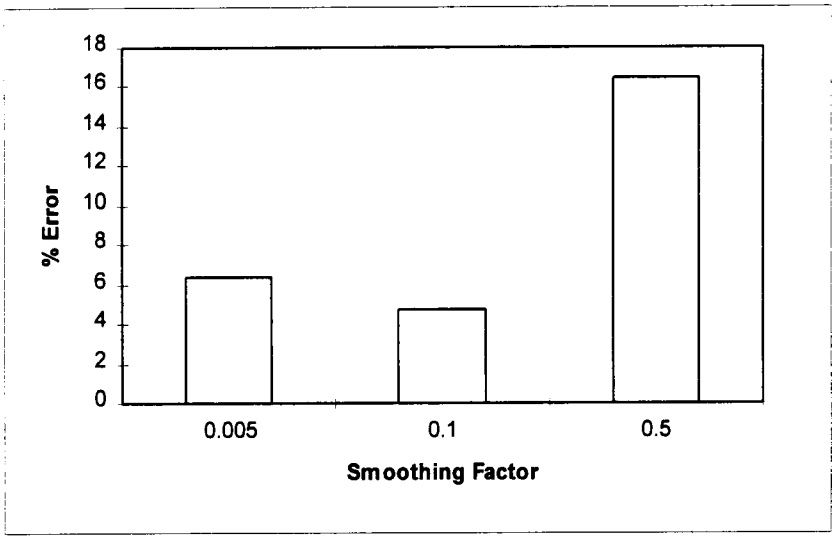


Figure 5.13: Effect of Smoothing Factor σ on PNN Classification Error.

Table 5.2: PNN classification results from testing set.

Class	Measurable	Non-measurable
Actual	132	65
Classified	134	63
True Positives	128	59
False Positives	6	4
True Positive Proportion	0.97	0.91
False Positive Proportion	0.09	0.03

5.3.4 Discussions

In AFIS waveform classification, only peak of the waveform is used to reject non-measurable fibers. It can effectively reject bundle fibers but peak only is not good enough to reject loop fibers. The use of multiple features from the whole waveform results in a better classification of the waveforms and thus ensure the accuracy of the length and diameter measurement.

Both PNN and decision tree classifier achieved good results in waveform classification. Although the same training set was used, the classification results were slightly different. The PNN tried to reduce the total classification error in training but the optimized tree classifier tried to reduce the classification error for measurable fibers, that is, less loop fibers are false classified as measurable fibers although a slightly more single fiber waveform may be classified as non-measurable class. This can be seen from the flow-chart of the decision tree classifier and it is the design intention to ensure the accuracy of the measurable class with a cost of lost a little more single fibers. Decision tree classifier also runs faster than PNN.

5.4 Optimization of Fiber Individualizer

5.4.1 Experiment Design

Two samples were used in optimization of fiber individualizer. The samples were tested on AL 100 for length and OFDA for diameter, which are listed in table 5.3. The sliver weight is about 6 g/m. 10,000 fibers were measured for each setting. The machine

settings are listed in table 5.4. Only one parameter will be changed at a time while the others are kept the same.

5.4.2 Results

The measure of optimization are short fiber content (% < 50mm), measurable waveform percent which defined as non-loop single fiber waveform, number-biased mean length and length CV%.

The results show that the pressure on apron has significant influence on length measurement. From the short fiber content for both samples, the 40x20 psi setting show significant fiber damages. 20x10 psi setting is the optimum setting for this test. Further lower the pressure to 10x5 was not successful because the pressure is not stable at this setting. Table 5.5 lists the results for pressure experiment. Output speed did not show significant influence on length measurement although the measurable fiber percentage show slight improvement when the output speed is reduced, therefore, higher output speed is recommended. The results are listed in table 5.6. The recommended drafting ratio for the first drafting zone is between 10 to 20 in order to keep web continuity. If we keep the total drafting ratio the same, reduce the drafting ratio on second draft zone will result in less measurable fibers and the mean length will get lower as shown in table 5.7. If the total drafting is changed, the result did not show that the higher drafting would result in better individualization. The measurable fiber percentage remains unchanged as shown in table 5.8. The result show that the higher drafting will increase the mean length but it is not easy to explain at this time, possibly, it related to fiber overlapping. From this

Table 5.3: Length and Diameter of the Sample

	AL Meter			OFDA	
Sample ID	Mean Length (Number)	CV %	% < 50 mm	Diameter (um)	CV %
1	79.7 mm	58.6	36.9	36.6 um	29.3
2	76.0 mm	48.5	30.9	21.72 um	25.4

Table 5.4: Parameters

	Parameters		
	Pressure *	Draft Ratio **	Output Speed
High	40x20 psi	20x700	450 rpm (1m /sec.)
Medium	20x10 psi	10x1000	250 rpm (0.5 m /sec.)
Low	10x5 psi	10x500	112 rpm (0.25 m /sec.)

* 40x20 psi: 40 psi for first apron, 20 psi for second apron.

** 20x700: 20 draft ratio for first draft zone, 700 draft ratio for second draft zone.

Table 5.5: Results from the Pressure Experiment

	Sample #1 (coarse)		Sample #2 (fine)	
Pressure	20x10 psi	40x20 psi	20x10 psi	40x20 psi
ML (n) (mm)	79.26	67.97	80.02	77.4
CV %	54.4	58.99	47.6	46.2
% < 50 mm	30.9	47.5	28.6	33.8

Table 5.6: Results from Speed Experiment

	Sample #1 (coarse)			Sample #2 (fine)		
Output Speed	112 rpm	250 rpm	450 rpm	112 rpm	250 rpm	450 rpm
ML(n)	79.78	79.70	81.14	80.15	80.02	79.26
CV%	46.56	47.68	47.99	44.76	44.17	44.68
%<50mm	28.9	30.9	30.6	29.8	28.6	30.7
Measurable Fiber %	80	79	77	71	72	70

Table 5.7: Results from drafting experiment to show the relationship between the first and second drafting zone.

	Sample #1 (coarse)	
Drafting	10x500	20x250
ML(n)	81.17	78.34
CV%	47.66	48.79
%<50mm	30.4	34.6
Measurable Fiber %	74	68

Table 5.8: Results from Drafting Experiment (total drafting)

	Sample #1 (coarse)		Sample #2 (fine)	
Drafting	10x500	10x1000	10x500	10x1000
ML(n)	81.14	82.33	80.02	81.05
CV%	47.99	47.9	44.17	43.94
%<50mm	30.9	29.4	28.6	28.7
Measurable Fiber %	79	78	72	72

experiment, 5,000 total drafting ratio is recommended. The best approach is to detect the mass or number and feedback to control the drafting depending on the sliver and the fineness of the fiber.

5.5 Evaluation of Length and Diameter Measurement

Nine samples with a wide range of length and diameter were used to evaluate of the performance of length and diameter measurement. Approximately 4,000 waveforms for each sample have been collected from the instrument. The results are listed in table 5.9. These samples were also tested by AL-meter for length and OFDA for diameter. Table 5.10 lists the results for these nine samples. The correlation between AL-meter mean length and new instrument mean length is high with $R^2 = 0.95$ as shown in Figure 5.14 (a) although the measuring principle is very different. (New instrument measures single fiber length while AL-meter measures the mass of the end-aligned bundle). The correlation between the new instrument mean diameter and OFDA mean diameter is also very high with $R^2 = 0.98$, but the CV% is higher than OFDA. Fiber orientation and crimp may have some influence on new instrument because it measures the shadow of the fibers.

Table 5.9: Length and Diameter of the samples measured by new instrument.

	Length (mm)		Diameter (um)	
Sample	L(n)	CV%	D	CV%
S1	83.4	51.38	35.24	26.75
S2	76.5	46.80	21.60	28.01
1901	77.0	47.79	27.73	25.88
3735	82.1	45.30	21.81	26.66
4764	90.6	42.75	22.50	26.34
3720	71.5	46.80	23.41	29.30
9345	73.8	48.56	18.02	30.40
3695	111.1	44.70	34.25	26.32
Blend	86.4	52.40	23.04	43.80

L(n)---mean length by number

CV%--- coefficient of variance

D ---- mean diameter

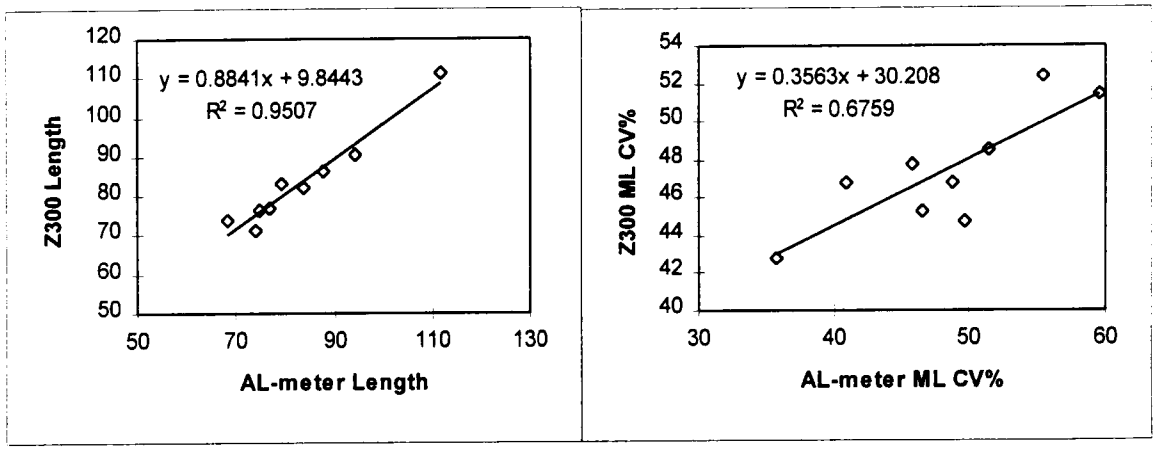
Table 5.10: Length and Diameter of the samples measured by AL-meter and OFDA.

	Length (mm)		Diameter (um)	
Sample	L(n)	CV%	D	CV%
S1	79.4	59.50	35.65	27.07
S2	74.6	48.80	21.57	22.13
1901	76.8	45.80	27.63	23.37
3735	83.9	46.50	22.09	21.43
4764	94.1	35.80	22.21	20.67
3720	74.1	41.00	23.48	21.53
9345	68.2	51.40	18.48	22.50
3695	111.9	49.80	34.98	26.53
Blend	87.8	55.40	20.83	37.40

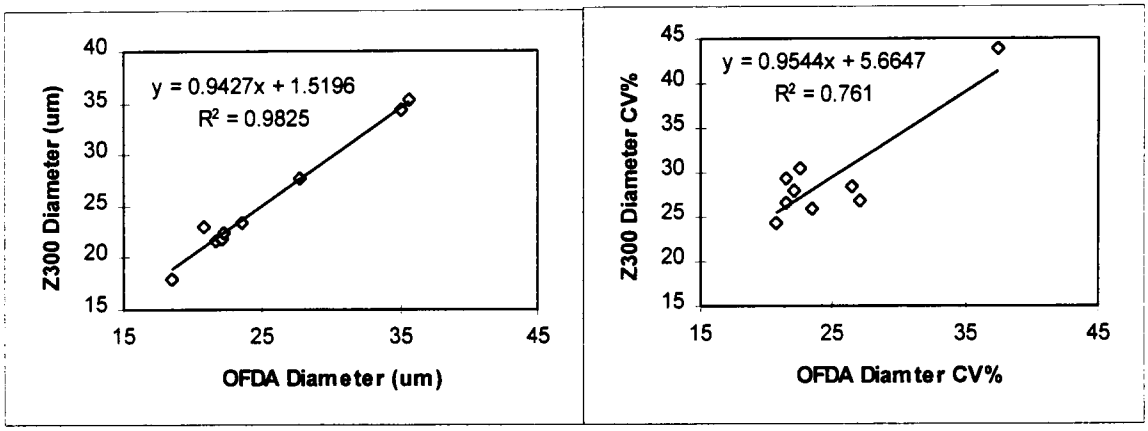
L(n)---mean length by number

CV%--- coefficient of variance

D ---- mean diameter



(a) (b)



(c) (d)

Figure 5.14: Comparison of length and diameter from new instrument with AL-meter and OFDA.

CHAPTER 6

WOOL TOP DEFECTS INSPECTION

Images of dark-fiber and vegetable matter were taken using the integrating cylinder described in chapter 4. Images of neps were taken on the same device with black background. Figure 6.1 illustrated some typical defects. Figure 6.1 (a) is an image of dark-fiber. The dark-fiber goes in and out of the web which brings difficulties to image analysis. Figure 6.1 (b) is a straw and (c) is a speck defect. Figure 6.1 (d) is an image with a nep, which is also not easy to detect.

The process of image analysis and measurement has many parts, and for convenience and clarity these will be dealt with one at a time, in more or less sequential order. Not all situations require all of these steps, but all are potentially available to deal with particular problems. They are summarized in Figure 6.2.

6.1 Image Processing and Measurement

6.1.1 Preprocessing

Image preprocessing encompasses a broad range of operations. The reason for these operations is usually to increase the visibility of some type of feature or information. It is also possible to use these operations to correct for known defects in the way the image was obtained, such as nonuniform illumination, or correcting an out-of-

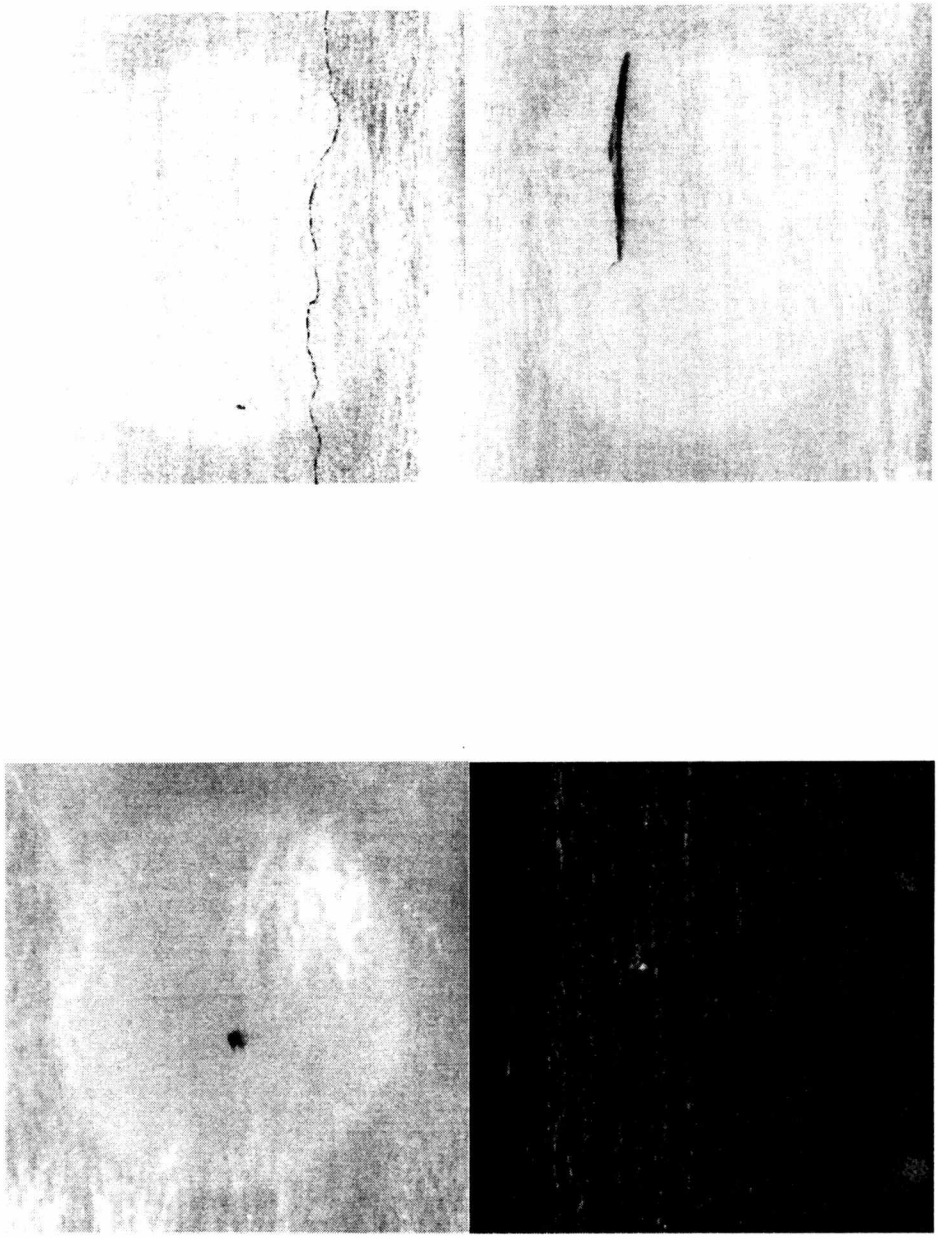


Figure 6.1: Images of defects among normal fibers, (a) dark-fiber, (b) straw, (c) specks, (d) nep.

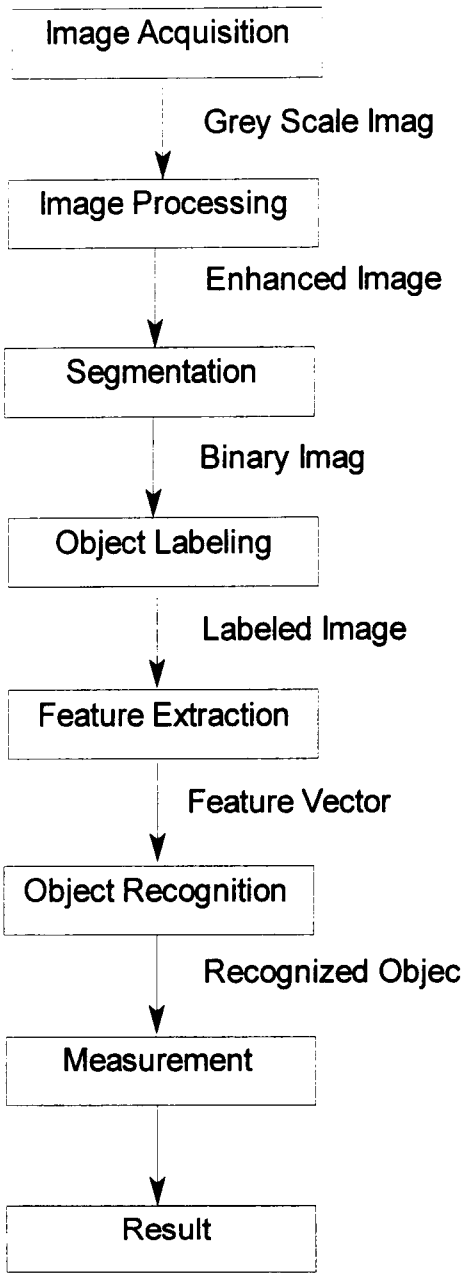


Figure 6.2: Flow chart of image processing and analysis.

focus condition or blur due to motion. The background of images in Figure 6.1 is not uniform. First step of preprocessing is to correct the background that is achieved by taking a blank image at the beginning of the testing and then correct the background by gain adjustment using this calibration image. The original images may have noise caused by digitization or another process applied to the image. Although noise cannot be eliminated altogether, it can be reduced by a process called smoothing. Because lowpass filtering will cause edge-blurring effect, median filter, in which we replace the gray level of each pixel by the median of the gray levels in a neighborhood of that pixel, is usually applied to a image to ensure edges remain crisp [43,44].

6.1.2 Thresholding

A binary image is distinct from a gray-scale image because each point is either white or black. Normally this is a guide to which points lie within the features we are interested in measuring, in other words, to separate figure from background. Binary images are often more suitable for measurement than gray scale images. However, they have lost all of the original brightness information.

The most common way of converting a gray scale image to a binary one is by thresholding. A thresholded image is created by defining

$$g(x,y) = \begin{cases} 1, & f(x,y) > T \\ 0, & f(x,y) \le T \end{cases}$$

where $f(x,y)$ is the gray level of point (x,y), T is the threshold and $g(x,y)$ is the thresholded gray level at point (x,y). Thus in examining $g(x,y)$, we find that pixels labeled 1 correspond to objects, while pixels labeled 0 correspond to the background. The

threshold T will be derived from the calibration. Figure 6.3 shows the thresholded images of Figure 6.1. Figure 6.3 (d) is a thresholded nep image, which is from the negative of the original image.

6.1.3 Blob Labeling

In many circumstances it is important to know whether two pixels are connected to each other and there are two major rules for deciding this. Figure 6.4 illustrates the two rules; 8-connected and 4-connected.

Once the binary image shows the separate objects present, then the next step is to check pixel connectivity and label each blob. 8-connectivity is used in the blob analysis process and each blob was labeled by gray levels. Figure 6.5 is an illustration of the labeling process of three blobs.

The labeling process defined region of interest (ROI). For each ROI, a set of features was selected which will be used for recognition of vegetable matter and dark-fibers.

6.1.4 Planer Shape Measures

Simple shape measures include area, perimeter, length, diameter, axes ratio, filling factor and circularity. These simple measures will be used in describe features for defects classification, therefore, they are discussed briefly here.

Area

Area is defined as the number of pixels contained on and within an object boundary.

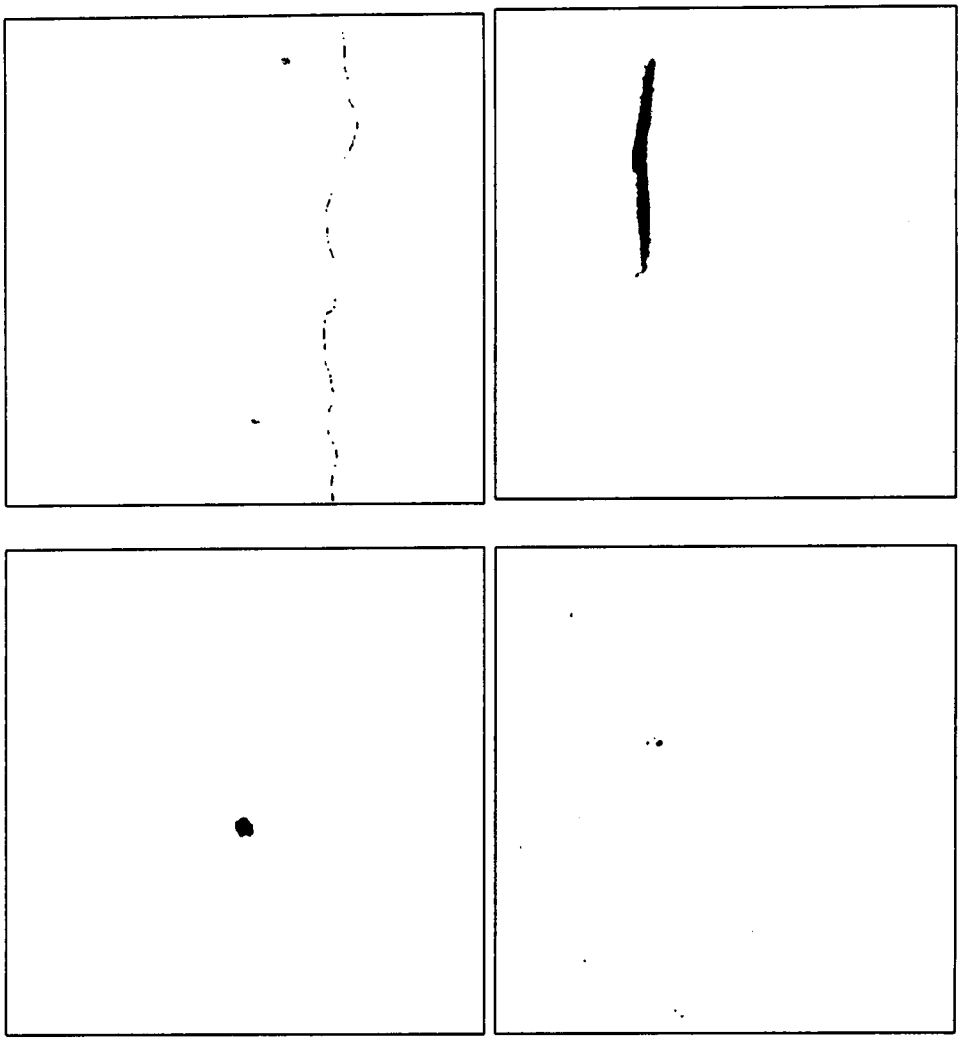


Figure 6.3: Thresholded images of figure 6.1.



(a) (b)

Figure 6.4: (a) 4-connectivity, (b) 8 connectivity.

```
  111
111111      2222      333
  111        2222     33333
              2222     33
```

Figure 6.5: Example of a labeling process.

Perimeter

Computing the perimeter of a region is a little difficult than computing its area. The perimeter of a region consists of the set of pixels that belong to the object and that have at least one neighbor that belongs to the background. Computing a perimeter of a region is a two step process.

Step 1:

Identify the boundary of a region. This can be accomplished by checking all the pixels in the region; for a 4-connectivity, if a pixel has three or less neighbors, mark it as a boundary pixel. The collection of marked pixels is object boundary.

Step 2:

Each pixel on the boundary and its neighborhood is checked to see which distance should be assigned to that pixel; if all neighbors are horizontal or all are vertical, the weight is 1; if all neighbors are diagonal, the weight is 1.414; if there is one diagonal and one nondiagonal neighbor, the weight is 1.207. All of these distances are summed to produce an approximate perimeter.

There are other algorithms to compute perimeter from a region. For example, a boundary can be extracted by dilating a region and then XOR the original one.

Length

Similar to perimeter, length can be computed by weighted distance between two pixels and then summed together.

Axes Ratio

The principal axis (PA) is defined as a line passing through the object's center of mass having a minimum total distance from all pixels belonging to the object. The steps to find a principal axis are as follows:

Step1:

Locate the center of mass.

Step 2:

Locate all boundary pixels that lie above the center of mass and mark them; the PA will pass through one of them and always passes through the center of mass; therefore, a set of lines that are candidates to be the PA; the center of mass is one point on these lines; and each of the marked boundary pixels represents another.

Step 3:

Compute the distance between each line and all of the pixels in the object and select the line having the smallest total distance as the PA.

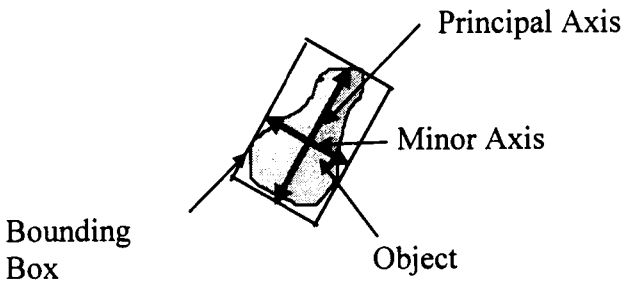
The minor axis is a line through the center of mass in a direction perpendicular to the PA. The Axes ratio is defined as the ratio of PA and MA.

Filling Factor

Filling factor is defined as the ratio of box area and object area as shown in Figure 6.6.

Circularity

The circularity is defined as



Axis Ratio = Major Axis / Minor Axis

Filling Factor = Object Area / Box Area

Figure 6.6: Illustration of axis ratio and filling factor.

$$Circularity = \frac{P^2}{4\pi A}$$

where P is perimeter and A is area of the blob. Circularity has a minimum value of 1.0 for a circle and increases, as the blob becomes more complicated.

6.2 Object Recognition and Feature Selection

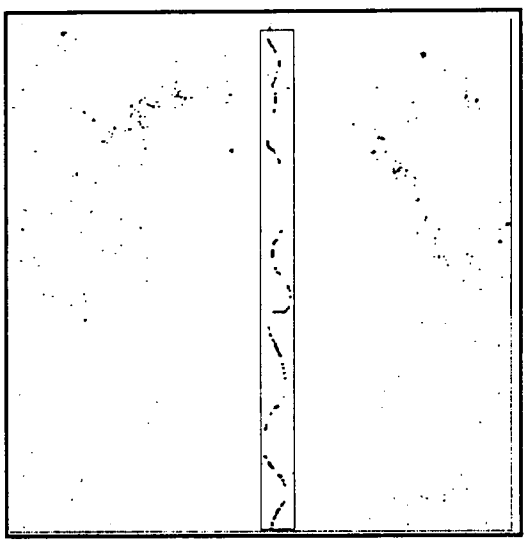
6.2.1 Object Recognition from a Noisy Background

Because dark-fibers and straws are interlaced with normal wool fibers in the thin web, they usually will show broken lines and dots in the thresholded image as shown in Figure 6.1 (a). Imperfect illumination and noise will make the situation even worse. Figure 6.7 (a) shows an image of dark-fiber in a noisy background. Although human eye can "see" fiber easily, it is not so easy for computer to find out the broken fiber in the noisy background. There is a number of clustering algorithms available, but most of them are not appropriate to use them directly. A special clustering algorithm was developed to find the line-like object in a noisy background. The algorithm has two steps. The first step is similar to single linkage algorithm.

Step 1: For each labeled blob, calculate the distance with its neighbors, if the minimum distance is smaller than a threshold, connect the blob with the minimum distance, otherwise, stop the searching. Figure 6.7 (a) illustrates the clusters. It is obvious some clusters are noises not the fiber/straw.



(a)



(b)

Figure 6.7: (a) Result of clustering. (b) Result of object recognition.

Step 2: For each clusters, calculate the scatterness of the cluster where scatterness is defined as the ratio of the number of blobs in the cluster divided by the total area of these blobs.

$$\text{scatterness} = \frac{N}{\sum_{1}^{N} Area_i}$$

where N is the total number of blobs and area is the area of each blob. For each cluster x_i, If the scatterness < threshold T, assign x_i to fiber/straw class, otherwise, assign x_i to noise class. The threshold T is determined by the training. Figure 6.7 (b) illustrates the classification results, where fibers are correctly recognized.

6.2.2 Features for Dark-fiber and Vegetable Matter Classification

Object recognition has two major components. The feature extractor gathers and organizes information concerning objects in the image. The classifier locates the most likely, best, or at least acceptable kind or class of objects, based on the features used. A feature is any measurement that is made on an image or region. Area, perimeter, circularity and orientation are basic features. There are several other ways to use features to describe an object. Some are perceived by a human observer and some are characteristic of the sample domain, yet not apparent to an observer. The Fourier descriptors have long been used for the purpose of either reconstructing or matching shapes [45]. The descriptors are defined as the Fourier series of contour points. Because of the properties of Fourier series, normalization with respect to location, scale, and rotation are easily achieved. However, the most difficult task in working with this approach lies in the lack of physical interpretations of high-order Fourier coefficients.

The method of moment invariants is another technique that has been used for shape description [46]. Statistical moment functions were derived and used to characterize the process of varying shapes though the use of shape signature.

In wool top defect inspection, the feature used in classifying dark-fibers, straws and specks/burrs are diameter, area, length, axes ratio, and filling factor. Diameter is a major feature to separate dark-fibers and straws. Length and filling factor will help the discrimination of fiber and straw also. Area, length and aspect ratio are good features for classification of straws, burrs and specks.

6.2.3 Features for Nep Classification

After thresholding, nep candidates were labeled by each blob. These blobs may be neps or not because the thresholded blobs are local fiber concentrations. Neps are knot-like fiber clusters but not the loose fiber clusters. Neps are usually have circular shape and have steeper slope in gray level gradient than loose fiber clusters. Figure 6.8 illustrates the slope difference in the cross section of nep and loose fiber cluster. To obtain both slope and shape information for each blob, the feature extraction process has two steps:

Step 1:

From thresholded image, compute the circularity for each blob.

Step 2:

From the thresholded image, find the location of the blob, then, from the same location in the original gray level image, compute the average slope.

The process of finding average slope is illustrated in Figure 6.9 where A_1 is the area of the blob and A_2 is the area of its neighborhood. The gray level difference of the two areas, G_1-G_2, gives an estimate of the average slope where G_1 and G_2 is the average gray level of A_1 and A_2 respectively. The reason for using square neighborhood is that it is faster in real-time processing and easier.

6.3 Defects Classification

6.3.1 Training and Testing Samples

Two samples having high dark-fiber content were used for dark-fiber / vegetable matter classification and another two samples having high nep content were used for nep detection. The samples were run on the drafting device and images were taken and stored for training and testing. 100 images were taken from the dark-fiber / vegetable matter sample set for dark-fiber / vegetable matter classification training and another 137 images were taken for testing. 25 images from nep sample set were used for training and another 40 images were used for testing. These images were inspected by a human operator and the defects were classified by visual judgment.

6.3.2 PNN Classifier

The same PNN classifier used in waveform classification was used in dark-fiber / vegetable matter classification. There are six inputs connect to six features. These are axis ratio, length, area, filling factor, diameter and scatterness. The three outputs correspond to dark-fiber class, vegetable matter and specks. Genetic algorithm was used to find the optimum smoothing factor σ in the training process.

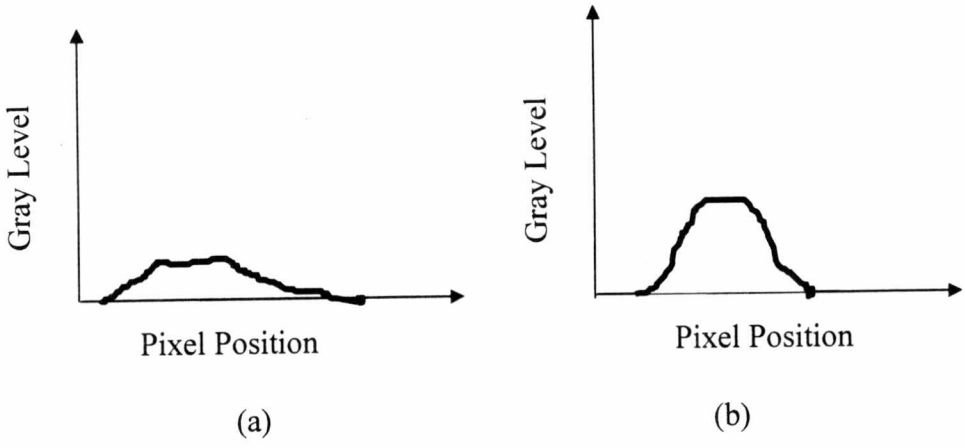


Figure 6.8: (a) cross-section of a loose fiber cluster. (b) Cross-section of a nep.

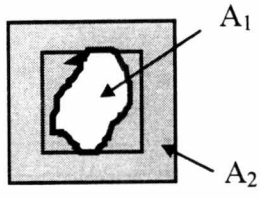


Figure 6.9: Illustration of blob area A_1 and its neighborhood area A_2.

6.3.3 Fuzzy Logic Classifier

Unlike conventional expert systems that use bivalent logic, fuzzy systems take a significantly different approach to machine intelligence and reasoning. A fuzzy system employs rules that accumulate evidence for a specific set of solution variables. Instead of isolating a point on the function surface, a fuzzy rule localizes a region of space along the function surface. When multiple rules are executed, multiple regions are combined in the same local space to procedure a composite region. The final point on the surface is found through defuzzification. Figure 6.10 illustrates the general organizational and flow schematic of a fuzzy reasoning system.

Input features are read into the system. Each rule is potentially executed. Some rules do not fire because their premise truth falls bellows the alpha threshold. Each rule that executes contributes some evidence about the value of its solution variable. This evidence, in the form of a fuzzy set, is correlated to agree with the truth of the premise and then aggregated into the on-going solution variable's fuzzy region. When all the rules have been fired, the composite solution variable's fuzzy set is defuzzified. This produces a number, the membership truth to the prototype pattern. Finally, the classification can be based on the membership truth-value. The heart of the fuzzy logic classification system is a set of fuzzy logic rules. The rules for identify dark-fiber, vegetable matter and neps are listed as follows:

- Dark-fiber:

1. If diameter is small, then dark-fiber potential is greatly increased.
2. If length is long, then dark-fiber potential is increased.

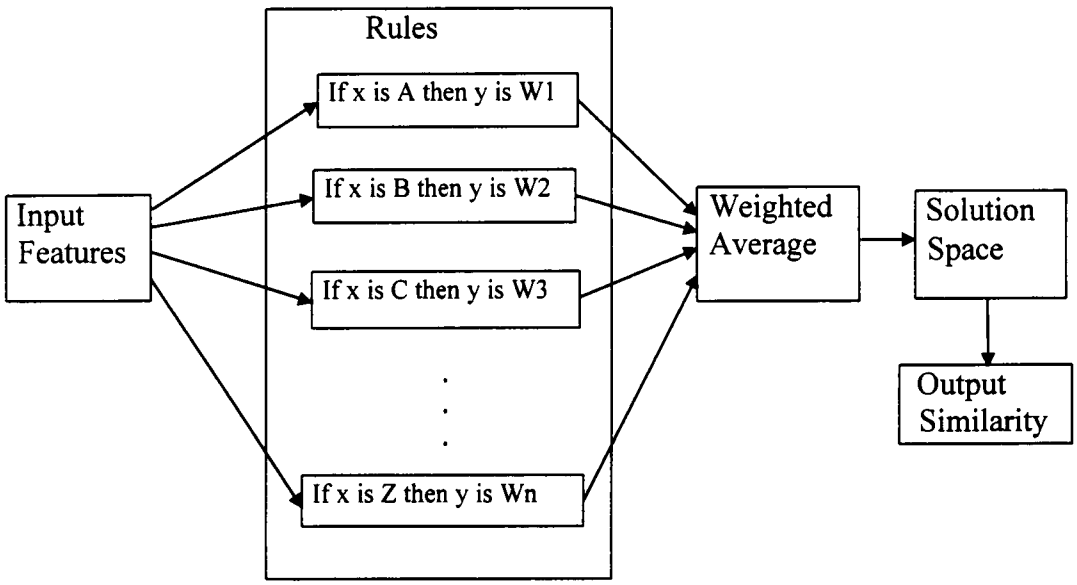


Figure 6.10: Fuzzy Reasoning System.

3. If scatterness is high, then dark-fiber potential is increased.

- Straw:

1. If diameter is large, then straw potential is greatly increased.

2. If length is short, then straw potential is increased.

3. If scatterness is low, then straw potential is increased.

- Burrs/Specks:

1. If filling factor is high, then burrs/specks potential is increased.

2. If axes ratio is low, then burrs/specks potential is increased.

- Nep:

1. If slope is high, then nep potential is greatly increased.

2. If circularity is around 1.0, then nep potential is increased.

The linguistic variables long, high, small, and around are fuzzy sets as illustrated in chapter 3.

Based on the rules described above, the fuzzy system employs a special kind of reasoning known as scaleable monotonic chaining. Scaleable monotonic chaining does not create and then defuzzify a solution fuzzy set. Rather, it uses monotonic chaining to map the potential specified in individual rules to an intermediate potential measuring fuzzy set. The result of this mapping is a scalar value from the domain of the potential metric indicating the degree of potential for this particular model factor. The monotonic reasoning results for each rule are weight averaged to produce a final potential value. The weight for each rule is trained by genetic algorithms similar to the process of optimization of thresholds described in chapter 5. This value is used to find the membership truth of the class evaluated. Figure 6.11 illustrates the process of nep

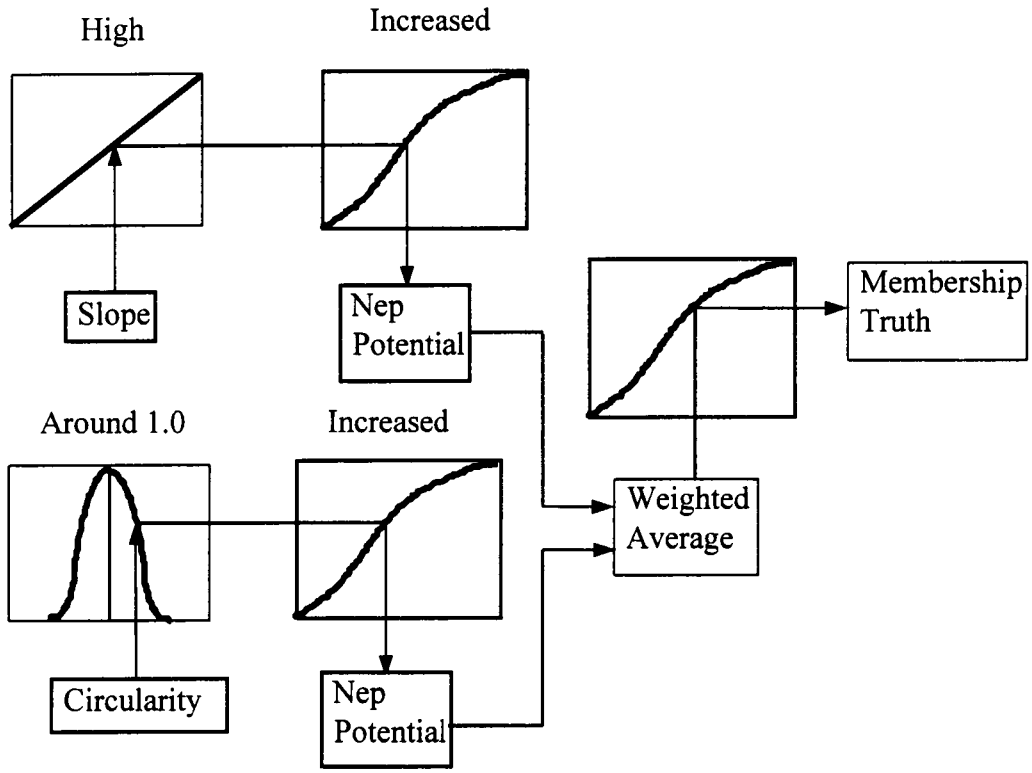


Figure 6.11: Fuzzy Reasoning for Nep.

classification. The complete classification system includes four fuzzy reasoning engines, one for each class, and a maximum selector. Given a feature vector, each fuzzy reasoning engine evaluates the feature vector and sends the membership truth-value to the maximum selector. The maximum selector assign the input feature vector to a specific class according to the maximum truth membership.

6.3.4 Results and Discussion

The dark-fiber / vegetable matter sample set were trained and tested by both PNN and fuzzy logic classifier. The nep sample set were trained and tested on fuzzy logic classifier only because there are only two inputs and quite simple. The results for dark-fiber / vegetable matter are listed in table 6.1 and 6.2. Both classifier show excellent results in classifying Burrs/Specks; there are 35 samples and all of them were classified right. The reason for excellent classification rate is the distinct shape difference for Burrs/Specks from other two classes. The true positive rate for dark-fiber and straws were not perfect because the overlapping region between them. Fine straws may be miss-classified into dark-fibers and coarse fibers may be miss-classified into straws also. The true positive rate are 0.95 and 0.81 respectively for dark-fiber and straws when using PNN. For the same testing set, the result from fuzzy logic classifier show slightly lower in dark-fiber class (0.92). The reason might be the third rule in dark-fiber classification is not appropriate. Most dark-fibers show high scatterness, but some of them may have very low scatterness. The total true positive rate for PNN is 0.93 and for fuzzy logic classifier is 0.91. Table 6.3 lists the classification results for nep using fuzzy logic classifier. There are 35 neps and 6 non-neps classified by human inspection from the images of the web

sample. Among the 35 neps, 34 of them were classified right and one was miss-classified as non-nep which result in a 0.95 true positive rate. The classification of non-nep has lower true positive rate. Two samples out of nine were classified as nep.

Table 6.1: PNN classification results for vegetable matter from testing set.

Class	Dark-fiber	Straws	Burrs/Specks
Actual	66	36	35
Classified	70	32	35
True Positives	63	29	35
False Positives	7	3	0
True Positive Proportion	0.95	0.81	1.00
False Positive Proportion	0.11	0.08	0.00

Table 6.2: Fuzzy logic classification results for vegetable matter from testing set.

Class	Dark-fiber	Straws	Burrs/Specks
Actual	66	36	35
Classified	68	34	35
True Positives	61	29	35
False Positives	7	5	0
True Positive Proportion	0.92	0.81	1.00
False Positive Proportion	0.11	0.14	0.00

Table 6.3: Fuzzy logic classification results for nep from testing set.

Class	Nep	Non-nep
Actual	35	9
Classified	36	8
True Positives	34	7
False Positives	2	1
True Positive Proportion	0.97	0.78
False Positive Proportion	0.06	0.11

CHAPTER 7

CONCLUSIONS AND RECOMMENDATIONS FOR FUTURE RESEARCH

7.1 Conclusions

A research prototype instrument for measuring major wool top properties was developed. This integrated system can measure wool fiber length distribution, diameter distribution and measure dark-fiber, vegetable matter and nep content. The length and diameter measurement was based on single fiber measurement. Single fiber measurement is technically superior than bundle fiber measurement because it is a direct measurement of distribution. The preliminary results show that both length and diameter measurement have excellent agreement with the commercial individual instrument. The results also show that the rejection of bundle fibers and loop fibers did not cause bias in measurement. Waveform recognition was based on the latest technologies in pattern recognition that ensures the accuracy of the measurement and is superior than the AFIS system used for cotton fiber. Defects inspection is based on digital image analysis technique. Satisfactory results were achieved in classification of dark-fiber, vegetable matter and neps.

The fiber individualizer is based on drafting principle. The results show that drafting can individualize the most of fibers as expected. The apron pressure, output speed and draft ratios are important parameters in optimization the performance of the individualizer.

Both physical and empirical models for length measurement were evaluated. The results show that the assumption of constant acceleration is appropriate in developing physical model. Using neural network to develop empirical model did not show significant improvement.

Various of classifiers were developed to classify waveforms and image objects which include probabilistic neural networks (PNN), optimized decision tree classifier and optimized fuzzy logic classifier. Although there are differences, all of them performed well in classification. The results show that smoothing factor is an important parameter in the performance of PNN classifier and threshold is an important parameter for decision tree classifier. For fuzzy logic classifier, the selection of fuzzy rules will determine the performance of the classification, which are based on the expert's knowledge. Because the selection of the classifier parameters is extremely important, genetic algorithms were applied to these classifiers to optimize the important parameters. The results show that genetic algorithms are good tools in solving combinational optimization problems.

One of the major difficulties in dark-fiber detection is that the dark fibers go in and out the web, which cause the broken segments in the image. Using clustering technique, these segments will be connected but it won't tell the difference between a fiber cluster and a background noise cluster. To identify the fiber cluster, a feature named "scatterness" was used. The results show this feature effectively separate the fiber cluster from noise cluster.

The classification error in classifying defects are mainly from dark-fibers and straws. In classification of dark-fibers and straws, diameter is an important feature but

diameter alone is not enough. Length and scatterness will have some help but not always correct.

In summary, the development of a research prototype instrument for wool fiber length and diameter distribution and defects inspection is successful. The feasibility of the measurement principal was proved.

7.2 Recommendations for Future Research

The direction of future research will towards the measurement of other wool fiber properties such as crimp, medullation, and color and fiber strength on the same integrated system.

The fiber individualizer can be further improved to control the individualization process. The drafting ratio may be automatically adjusted based on the detection of feeding sliver weight. The settings for apron pressure may need further refinement.

The integrating cylinder need to be further improved to provide more uniform illumination.

Features for waveform recognition and defects classification need further refinement. Other image preprocessing and segmentation techniques may be tried to provide better images for analysis.

The probabilistic neural network developed was based on a single smoothing factor σ. For further improvement of PNN, separate σ for each variable might be used.

Recently there is a common theme among fuzzy researchers: how can we create a fuzzy system from the underlying databases of information. This approach would solve several problems: it would discover and create the fuzzy sets and it would form and write

the actual system rules. Therefore, automatic generation of fuzzy logic rules for classification from the training samples might be tried using Wang-Mendel algorithm of rule discovery method and then the rules might be selected by the genetic algorithms [49].

BIBLIOGRAPHY

BIBLIOGRAPHY

1. Anderson, S.L., "The measurement of fiber fineness and length: the present position." J. Text. Inst. 67:175-180, 1976.

2. Lamb, P.R., "The effect of fiber diameter distribution on yarn properties," Wool Tech, Speep. Bdug, 40, 1992.

3. IWTO-17-85, Determination of Fiber Length Distribution Parameters by Means of the Almeter, The International Wool Secretariat, Valley Drive, Ilkley, West Yorkshire LS29 8PB.

4. IWTO-47-95, Measurement of the Mean and Distribution of Fiber Diameter of Wool Using an Optical Fiber Diameter Analyzer (OFDA), The International Wool Secretariat, Valley Drive, Ilkley, West Yorkshire LS29 8PB.

5. IWTO-12-95, Measurement of the Mean and Distribution of Fiber Diameter Using the Sirolan-Laserscan Fiber Diameter Analyzer, The International Wool Secretariat, Valley Drive, Ilkley, West Yorkshire LS29 8PB.

6. IWTO-6-92, Method of Test for the Determination of the Mean Diameter of Wool Fibers in Combed Sliver Using the Airflow Apparatus, The International Wool Secretariat, Valley Drive, Ilkley, West Yorkshire LS29 8PB.

7. IWTO-8-89, Method of Determining Fiber Diameter and Percentage of Medullated Fibers in Wool and Other Animal Fibers by the Projection Microscope, The International Wool Secretariat, Valley Drive, Ilkley, West Yorkshire LS29 8PB.

8. IWTO-13-88, Counting of Colored Fibers in Tops by the Balanced Illumination Method, The International Wool Secretariat, Valley Drive, Ilkley, West Yorkshire LS29 8PB.

9. IWTO-24-73, General and Specific Methods for the Determination of Cleanliness Faults in Combed Wool Slivers, The International Wool Secretariat, Valley Drive, Ilkley, West Yorkshire LS29 8PB.

10. ASTM-D1770-88, Standard Test Method for Neps, Vegetable Matter, and Colored Fiber in Wool Top, ASTM Standards, Vol. 07.01.

11. Breiman, L., Olshen, R.A. and Stone, C.J., Classification and Regression Trees, Wadsworth, 1984.

12. Quinlan, J.R., "Induction of Decision Tree," Machine Learning, Vol.1, pp. 81-106, 1986.

13. Meisel, W.S. and Michalopoulos, D.A., "A partitioning algorithm with application in pattern classification and the optimization of decision trees," IEEE transactions on Computers, Vol. c-22, No. 1, 1973.

14. Hertz, J., Krogh, A. and Palmer, R.G., "Introductions to the Theory of Neural Computation," Addison-Wesley, Reading, MA, 1991.

15. Maren, A., Harston, C. and Pap, R., "Handbook of Neural Computing Applications," Academic Press, Inc., 1990.

16. Simpson, P. K., "Artificial Neural Systems," Pergamon Press, New York, 1989.

17. Khanna, T., "Foundations of Neural Networks," Addison-Wesley, New York, 1990.

18. Taylor, M. and Lisboa, P., "Techniques and Application of Neural Networks," Ellis Horwood, New York, 1993.

19. Hecht-Hielsen, R., "Theory of the Backpropagation Neural Network," Intl. Joint Conf. on Neural Networks (Washington), vol. I, pp593-605, 1989.

20. Rumelhart, D.E., Hinton, G., and Williams, R.J., "Learning Internal Representations by Error Propagation, " Parallel Distributed Processing, Vol. 1, MIT Press, Cambridge, MA, 318-362, 1986.

21. Kohonen, T., Self-Organization and Associative Memory, Springer-Verlag, Berlin, 1984.

22. Fukunaga, K., "Bayes Error Estimation Using Parzen and k-NN Procedures," IEEE Transactions on Pattern Analysis and Machine Intelligence, 9: 634-643, 1987.

23. Specht, D., "Probabilistic Neural Networks for Classification, Mapping, or Associative Menory," IEEE International Conference on Neural Networks, San Diego, CA, 1988.

24. Specht, D., "Probabilistic Neural Networks," Neural Networks, 3: 109-118. 1990.

25. Specht, D., "Enhancements to Probabilistic Neural Networks," International Joint Conference on Neural Networks, Baltimore, MD. 1992.

26. Specht, D., and Shapiro, P.D., "Generalization Accuracy of Probabilistic Neural Networks Compared with Back-Propagation Networks," Lockheed Missiles & Space Co., Inc. Independent Research Project RDD 360, I-887-I892, 1991.

27. Holland,J.H., "Adaptation in Neural and Artificial Systems," Ann Arbor, Mich.: University of Michigan Press, 1975.

28. Davis, L., "Genetic Algorithm and Simulated Annealing," Morgan Kaufmann Publishers, Inc., Los Altos, California, 1987.

29. Glodberg, D.E., "Genetic Algorithms in Search, Optimization, and Machine Learning," Addsison-Wesley, New York, 1989.

30. Muselli, M. and Ridella, S., "Supervised Learning Using a Genetic Algorithm," INNC-90-Paris: Vol.2, pp. 790. Paris, France, July, 1990.

31. Booker, L. B., Goldberg, D.E., and Holland, J.H., "Classifier Systems and Genetic Algorithms," Artificial Intelligence, 40: 235-282, 1989.

32. Davis, L., "Handbook of Genetic Algorithms," Van Nostrand Reinhold, New York, 1991.

33. Kosko,B., and Isaka,S., "Fuzzy Logic.", Scientific American (July), 76-81, 1993.

34. Terano, T., Asai, K., and Sugeno, M., Fuzzy Systems Theory and Its Applications, Academic Press, San Diego, CA, 1991.

35. Zadeh, L.A., and Kacprzyk, J., Fuzzy Logic for the Management of Uncertainty, John Wiley and Sons, New York, 1992.

36. Cox,E.D., "Approximate Reasoning: The Use of Fuzzy Logic in Expert Systems and Decision Support." Proceedings of the Conf. on Expert Systems in the Insurance Industry, New York, April, 1991.

37. Kosko,B., Fuzzy Thinking: The New Science of Fuzzy Logic, Hyperion, New York, NY, 1993.

38. Bragg,C.K., "Advanced Technology for Measureing Cotton Fiber Length Diameter and Trash Content.

39. ASTM-D5866-96, Standard Test Method for Nep in Cotton, ASTM Standards, Vol 07.01

40. Lord, P.R., and Grover, G., Roller Drafting, Textile Progress, The Textile Institute, Vol. 23, No.4, 1993.

41. Chudleigh, P.W., "Detecting Colored Contaminants in Wool Using an Integrating Sphere," Textile Res. J. 61(10), 568-574 (1991).

42. Chu,Y.T., Private Report, Zellweger Uster Inc., 1996.

43. Gongalez, R.C. and Wintz, P., Digital Image Processing, Addison-Wesly, Reading, Massachusetts, 1977.

44. Jain, A.K., Fundamentals of Digital Image Processing, Prentice Hall. Englewood Cliffs, New Jersey, 1989.

45. Persoon, E. and Fu, K.S., "Shape Descrimination Using Fourier Descriptors," PAMI, Vol. 8, No. 3, 388-397, May 1977.

46. Zhu, M., Hasani, S., Bhattarai, S. and Singh, H., "Pattern Recognition with Moment Invariants on a Machine Vision System," Pattern Recognition Letters 9 175-180, 1989.

47. Wang, L.X., and Mendel, J. M., "Generating Fuzzy Rules from Numerical Data, with Applications.", USC-SIPI Report No. 169, Signal and Image Processing Institute, University of Southern California, Los Angeles, CA, 1991.

VITA

Luo Cheng (Cheng Luo) was born in Shanghai, P. R. China, on March 30, 1959. He graduated from China Textile University (CTU), Shanghai, in 1982 with a Bachelor of Science degree in Textile Engineering. From 1982 to 1985, he was employed by CTU as an instructor and research associate in the Dept. of Textile Engineering. During that time, Luo was primarily engaged in the research of Air-jet spinning, carding and textile instrumentation. Also, he was responsible for the laboratory courses in Textile Engineering. In January 1986, Luo Cheng entered the Graduate School of the Kansas State University. One year later, he transferred to The University of Tennessee at Knoxville and received Master's degree with a major in Textile Science and a minor in Electrical Engineering in May 1989. In 1990, he accepted a job offer from Motion Control Inc. in Dallas, Texas, as a research engineer. From that time, his research was focused on textile instrumentation. Luo Cheng moved back to Knoxville in 1995. He was employed full-time by Zellweger-uster as a research engineer and continued his study at The University of Tennessee as a part-time graduate student pursuing Ph.D. degree. In December 1997, he received Doctor of Philosophy degree with a concentration in Textile Science and minor in Electrical Engineering.